LAPPEENRANTA UNIVERSITY OF TECHNOLOGY
School of Energy Systems
Department of Environmental Technology
Sustainability Science and Solutions

Mohammad Naji Nassajfar

CFD Simulation of Electric Vehicle Thermal System and Investigation of Thermal Insulation for Cabin

Examiner: Professor Risto Soukka

Supervisors: M.Sc. Magdalena Klotz
Ph.D. Mohammad El-Alti

ABSTRACT

Lappeenranta University of Technology
LUT School of Energy Systems
Degree Programme in Environmental Technology
Sustainability Science and Solutions

Mohammad Naji Nassajfar

CFD Simulation of an Electric Vehicle Thermal System and Investigation of Thermal Insulation for Cabin

2018

75 pages, 46 figures, 17 tables

Examiner: Professor Risto Soukka

Supervisors: M.Sc. Magdalena Klotz
Ph.D. Mohammad El-Alti

Keywords: sustainable mobility, 1D CFD simulation, 3D CFD simulation, electric vehicle, thermal management, GT-Suite, Star-CCM+, energy saving

Heat generated in combustion engine is mainly considered as waste and the task of thermal management system of vehicle was to efficiently conduct waste heat away from the combustion engine. However, there is much less heat generated by the electric motor and thermal management is different in electric vehicle (EV). Powertrain, traction battery and passenger's compartment are three main subsystems where heating, cooling and climate control system should be considered to provide efficient thermal conditioning. In this thesis, the thermal subsystems of the EV are modelled and integrated via 1D simulation using GT-Suite program to obtain a thorough study of heat loss within the vehicle. In 1D simulation, the performance of the system in both cooling and heating modes and in three use cases of 40, 80 and 120 kph are investigated. Based on the results of the 1D analysis, glass boundaries of cabin have the highest heat loss and incorporate high potential for energy saving. Thereafter, two insulation solution for cooling and heating modes are proposed and investigated in 3D simulation using Star-CCM+ program. As the final step insulation solutions are compared regarding energy saving, weight and commercial feasibility. This thesis work is done in collaboration with NEVS AB, Trollhättan, Sweden.

ACKNOWLEDGEMENTS

I would like to take this opportunity to thank Almighty God for his guidance in my whole life and to achieve my academic goals. It was my honor to be involved in this master thesis project. Experts at NEVS AB have been very welcoming, friendly and helpful throughout my thesis project. They have supported me with their comprehensive expertise and knowledge of automotive systems. I have gained a lot from this thesis. Not only the knowledge in thermal management systems but also the innovate spirit to solve complex problems.

I would also like to thank my supervisor Magdalena Klotz and Mohammad El-Alti for their warm and friendly support. With a heart full of gratitude, my salutation goes to all engineers in the Thermal Management department, namely to Shkelzen Plakiqi, Claes Zimmer, Leif Eriksson, Jonas Gunnarsson, Kristian Abdallah and Dai Kaixiang for attending my presentation and giving many valuable suggestions and opinions.
I would like to thank my examiner Professor Risto Soukka at Lappeenranta University of Technology for his directions and cooperation.

From the bottom of my heart, I would like to thank my wife Saeideh, who taught me how to love and gave me her infinite support in every single moment of our life. Finally, a warmth thanksgiving goes to my family for their prayers and help, without them I could never be in this position.

TABLE OF CONTENTS

List of Figures

List of Tables

Abbreviations

1D	One Dimensional
3D	Three Dimensional
AC	Air Conditioning
CFD	Computational Fluid Dynamics
EEA	European Environment Agency
EV	Electric Vehicle
HTC	Heat Transfer Coefficient
HVAC	Heating, Ventilation, Air-Conditioning
ICE	Internal Combustion Engine
KPH	Kilometer Per Hour
NEVS	National Electric Vehicle Sweden
RESS	Renewable Energy Storage System
TM	Thermal Management

1 INTRODUCTION

This chapter presents a summary of the thesis. Section 1.1 defines the motivation of this report. Section 1.2 describes the problem to be solved. Section 1.3 explains the objectives and deliverables required for successful outcome of this report. Finally, section 1.4 points out the restrictions of this thesis.

1.1 Background

The mobility sector in 2015 was responsible for 30% of the total EEA-33 countries primary energy consumption. Furthermore, this sector is the second highest greenhouse gas producer and accounted for 34% of the CO2 emissions mainly generated from fossil fuels combustion (EEA, 2017).

Contribution of Electric Vehicles in market is expected to increase significantly in near future. By 2020, about 2.5 million EVs will enter U.S market based on studies carried out by the University of California, Berkeley (Becker and Sidhu, 2009). Energy required for HVAC system in EV supplies from stored energy in battery system and decreases the vehicle driving range specifically in extreme climate condition. Driving range is an important indicator for evaluating the performance of EV. ‘Range anxiety’ is a critical issue for battery electric vehicle drivers, specifically for unskilled drivers according to Rauh, Franke and Krems, 2014. HVAC system counts as one of the major energy consuming parts of EV. In (-18 C) ambient temperature, the energy consumption in in heating system decreases the driving range to 43% of regular value, see figure 1.

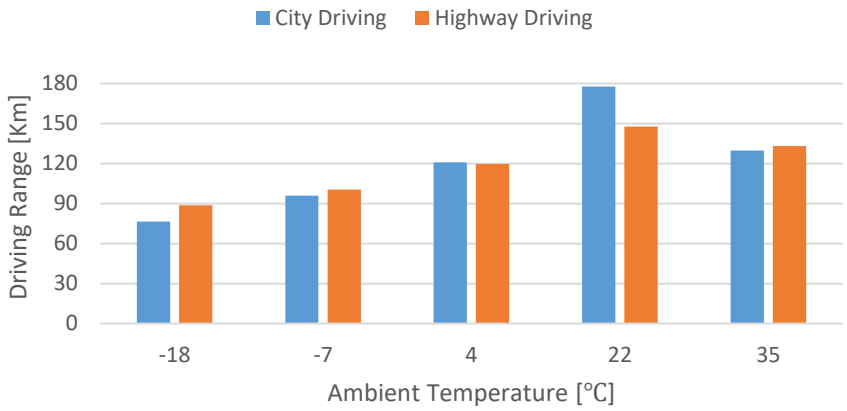

Figure 1. Effect of ambient temperature on driving range of Nissan Leaf, HVAC system turns off in 22°C (Stutenberg, 2014).

1.2 Problem Definition

The definition of thermal system of EV is agreed on as follows: It is a system incorporating all physical energy draining/gaining components of the Saab 9.3 based EV. Definition of physical system is presented in second chapter of thesis and shown in figure 3 of chapter 2. The diagram depicts thermal system of EV and main problem is to find out the heat loss in the system.

Electric vehicle thermal system includes 3 subsystems: Powertrain Unit, Battery system and Passengers compartment. The second chapter of this thesis is dedicated to defining the key elements of EV thermal system. These subsystems are connected with hoses and pipes. The question is how much is heat loss in each subsystem for specific use case. Heat loss is defined as the thermal energy generated from battery source and transferred to ambient air. The next question is how to insulate the area with highest heat loss using suitable insulation solutions.

1.3 Objectives

To achieve the objectives of this thesis, I proceeded as follows to maintain cohesion from assignment definition to final solution evaluation. This chapter defines the primary assignment and continues to set objectives and deliverables. Objectives and the main goal are discussed in chapter 1.3.2. Figure 2 shows the outline of this thesis.

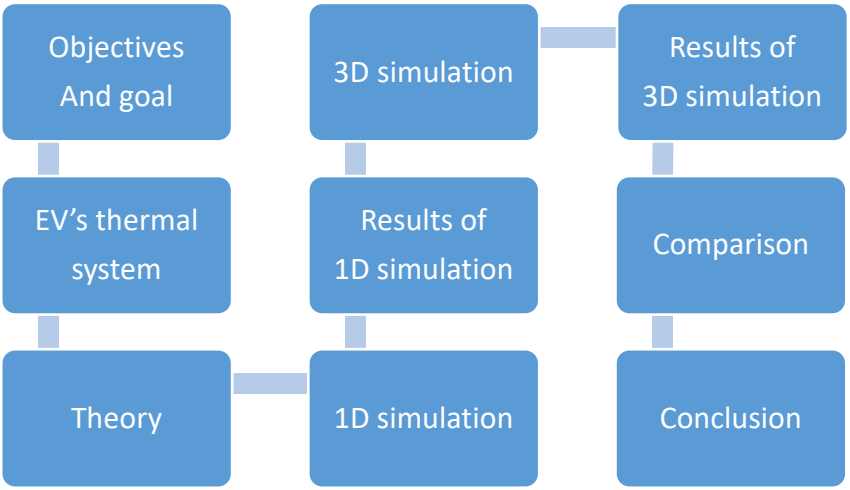

Figure 2. Chain process of the assignment.

1.3.1 Thesis Assignment

The Thesis project was assigned to me on February 2018 with the following objectives:

Table 1. Assignment of Thesis project.

Project Title	**CFD Simulation of Electric Vehicle Thermal System and Investigation of Thermal Insulation for Selected Area**
Defined objectives	Familiarizing with the Thermal Management system of EV
	1D Simulation of EV thermal system using GT-Suite
	3D Simulation of chosen area using Star-CCM+
	Investigation of suitable thermal insulation for selected area

1.3.2 Objectives and the Main Goal

Regarding the Thesis assignment, the main goal and objectives are set to fulfil the requirements of both Lappeenranta University of Technology and NEVS AB. Table 2 elaborates the goals and objectives of this project.

Table 2. Main Goal and Objectives of the Thesis.

Main Goal	Determine heat loss in each subsystem of EV and propose thermal insulation for selected area
Objective 1	Identify relevant use cases
Objective 2	Determine position of each component in specific use case.
Objective 3	Develop the 1D model in GT-Suite for entire system
Objective 4	Determine heat loss in each sub-system

Objective 5	Select the subsystem for further investigation
Objective 6	Simulate the area with highest heat loss in Star-CCM+
Objective 7	Assessment of insulation solutions

1.4 Limitations

The results of simulation are highly dependent on the input values and defined boundary conditions. Thermal system of EV contains numerous components which should be defined correctly to obtain reliable results. In addition, the models should be calibrated with testing. In this study fluid flow is considered to be steady and heat transfer is transient. The result of simulation is only valid for the NEVS specific architecture.

2 COMPONENTS OF THERMAL SYSTEM

Components of thermal system are the parts that effect the thermal behavior of TM system without consideration of the physical shape of the system in EV. The goal of classification is to discriminate the components and to categorize elements of each subsystem. Hence, 4 main components in thermal system of EV are:

- **Powertrain unit**
- **Battery System**
- **HVAC System**
- **Passengers Compartment (cabin)**

The overall schematic of thermal system in EV is demonstrated in figure 3. The connecting arrows symbolize direct thermal energy interaction between components. Transferred heat between battery box and cabin is excluded from the system due to marginal value.

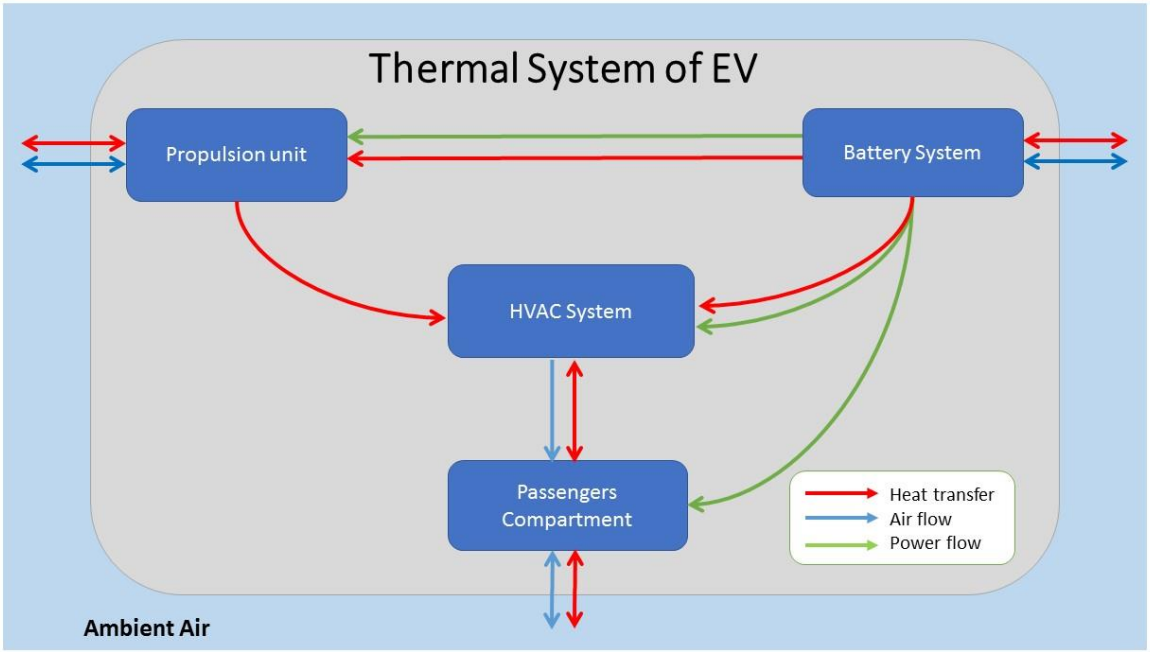

Figure 3. Schematic model of Thermal Management System in EV.

2.1 Logical Subsystems of the Key Components

This chapter describes logical subsystems of the key components that have major influence on the thermal management inside EV. In this thesis, only the components with either high energy consumption or significant heating/cooling demands (over hundreds of kW) were considered for the final design of TM system.

2.2 Powertrain (propulsion) Unit

In powertrain unit motor and invertor generate heat and in every condition this loop needs to be cooled down. Propulsion unit of EV transforms electrical energy received from Battery cells into kinetic energy to propel the vehicle. Figure 4 below shows components of Nissan Leaf e-powertrain. Main parts of powertrain cooling system are motor, power electronics and pump.

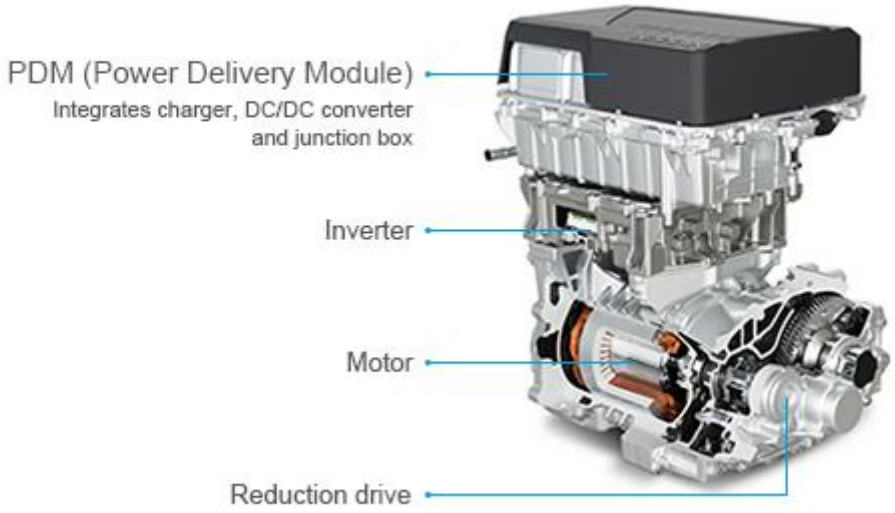

Figure 4. Electric powertrain of electric vehicle. (NISSAN MOTOR Co., 2018)

2.2.1 Electric Motor

Electric motor consumes the stored energy in battery and propels the vehicle's wheels. The process of converting electrical energy to kinetic energy in components of an electric powertrain generates heat. The task of thermal management system is to reduce the working

temperature of the electric motor to guarantee high performance and long lifespan for the electric motor.

The typical approach of e-motor cooling is by applying fins mounted on the outer surface of the electric motor shell. The fins function is to expand the surface of the motor shell and enhance the value of convective heat transfer from the surface of electric motor to the ambient air. (Putra, N. 2017)

2.2.2 Coolant Motor

Powertrain coolant motor drives the coolant in propulsion cooling system as all the part, even pipes, have pressure loss that requires to be overcome. In ICE vehicles, the pumps have mechanical connection to the engine shaft which maintain a fixed pump speed, however, in electric cars the coolant motors are electric driven. Figure 5 shows an electric coolant pump made by Continental automotive.

Figure 5. Electric coolant pump. (Continental-automotive, 2018)

2.2.3 Power Electronics

This part is responsible for regulating electrical energy directing from battery pack to electric motor. Power electronics system is affected by temperature and requires specific temperature band to run optimally. Propulsion coolant loop absorbs the generated heat in power electronics and provides appropriate temperature for electronic chips.

2.3 Battery System

Battery System stores and deliver electrical energy to other subsystems of EV. Thermal management of EV's battery is essential to maintain the EV's range and battery reliability. The most efficient working temperature for a lithium-ion traction battery is almost the same temperature that is proper for human body and thermal systems needs to warm/cool the battery (Porsche engineering magazine, 2011). Ambient temperature as well as internal heat generated in battery are considered as players of thermal management for the battery system. Low temperature decreases the power output because of suppression in electro-chemical reactions, while high temperature elevates corrosion causing lower battery life (Jarrett and Kim, 2011). Figure 6 shows traction battery and coolant pipes of Chevrolet Bolt EV. Components of Battery system are battery modules, DC-DC converter, on-board charger, sensors and RESS box.

Figure 6. Chevrolet Bolt EV Battery. (Chevrolet, 2018)

2.3.1 Battery Modules

Most of automobile manufacturers utilize Lithium-ion battery cells due to high power density and availability in the market. High cost of cells as well as environmental concerns, make the maximization of lifetime desirable by the both producers and consumers. Aging of lithium-ion batteries is not only affected by time, also the state of charge (SOC), charge-discharge rate (C-rate), the depth of discharge (DOD) and more importantly extreme temperatures decrease the lifespan. Maintaining functional temperature in the range of 25 to

35 °C while acquiring a uniform temperature inside battery cell packs (modules) aids limit aging. (Smith et al., 2014)

Heat source in batteries can be divided into three basic concepts of reaction, joule and polarization heat generation. Reaction heat is generated in the chemical reactions during charging and discharging processes. Joule heat is produced due to electrical resistance and is associated to electrical performance of cells. Polarization is related to energy loss of electro-chemical polarization in battery cells (Sato, 2001).

2.3.2 DC-DC Converter

This device is utilized to provide low-voltage DC power for charging 12V battery to operate EV accessories.

2.3.3 On-board Charger

It converts AC electricity supplied form stationary charging port into DC to charge the traction battery.

2.3.4 Sensors

They are used to measure temperature of battery modules in RESS box. Coolant flows through battery modules consecutively and surface temperature of modules are dissimilar. Thus, it is essential to measure temperature of every single module to control the cooling system.

2.3.5 RESS Box (Rechargeable energy storing system)

RESS box protects battery modules and preserves temperature conditioning for the battery modules. The battery pack in made of PVC materials and covers all battery system. It is located under the cabin and isolates the battery system from moisture and harsh temperature.

2.4 HVAC and AC System

HVAC system is the most significant element of EV's thermal management system. It provides suitable operating temperature range for the Propulsion unit, Battery System and passengers' compartment. Main duties of HVAC system are: Heating, Ventilation, Cooling, Dehumidification and air cleaning. Figure 7 demonstrates components of HVAC unit. The required components to achieve mentioned duties are listed below.

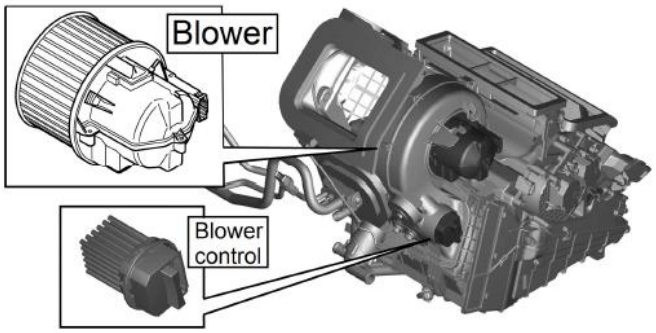

Figure 7. Components of HVAC unit. (Nielsen, F. 2016)

2.4.1 Evaporator

It is a heat-exchanger which absorbs heat from surrounding air and transfer it to the refrigerant in the inner fins. In addition, it dehumidifies the air by condensing the moisture content of air on its surface.

2.4.2 Condenser

A heat exchanger (radiator) as shown in figure 8, is located in front of vehicle and releases the absorbed heat in the gaseous refrigerant and changes its state to liquid.

2.4.3 Compressor

The function of compressor is to compress the gaseous refrigerant to superheat vapor whilst circulating the refrigerant in AC system.

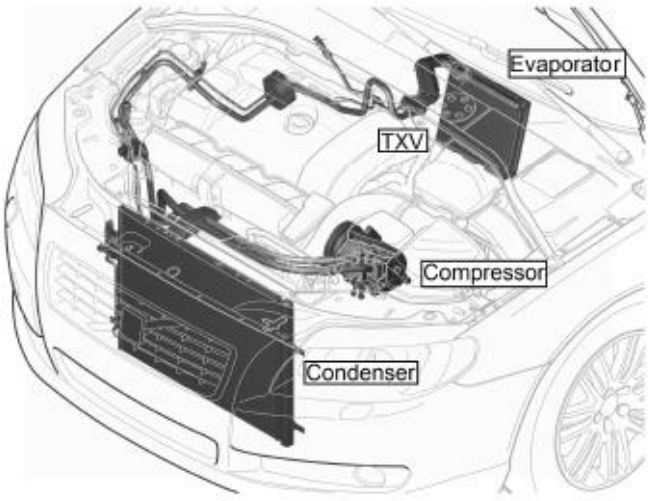

Figure 8. Components of AC system. (Nielsen, F. 2016)

2.4.4 Expansion Valve (TXV)

It reduces the refrigerant pressure from high to lower state to regulate the superheat point of refrigerant in evaporator. Figure 8 above demonstrates the position of TXV valve in refrigerant loop.

2.4.5 Accumulator

Protects the performance of compressor by separating the liquid part of refrigerant which did not convert to vapor in the evaporator.

2.4.6 Heater

The task of electric heater is to heat up the coolant for further distribution of heat into cabin or battery system in cold ambient temperature.

2.4.7 Refrigerant/Coolant

Refrigerant and coolant are fluids used to carry heat in HVAC system. The coolant in the entire system is a 50-50 mixture of water and antifreeze. The refrigerant in the system is R-134a.

2.4.8 Pipes and hoses

Rubber hoses and Aluminum pipes serve the duty of distribution of coolant and refrigerant respectively through HVAC system. The temperature in the coolant and pressure in refrigerant system can be high; therefore, they should be designed in a way to resist different operational conditions.

2.4.9 Fan

Fans assist the heat-exchangers to dissipate the absorbed heat by forcing the air through Heat-exchangers fins. Additionally, the HVAC blower guides the ambient air through HVAC module and compartment. Figure 9 shows the position of fan in TM system.

Figure 9. Position of fans in Air-conditioning loop. (Valeo, 2018)

2.4.10 Vents

Vent is outlet terminal of duct lines which connects HVAC system with compartment, battery system and ambient air and regulate the inlet and outlet air flow.

2.4.11 Filter

Filter as shown in figure 10, is placed at the inlet of HVAC module and separates contaminant particles from air.

Figure 10. Cabin filters. (Valeo, 2018)

2.4.12 Air Distributor

The function of air distributor conduit as shown in figure 11, is to distribute air through vents according to desired air flow and temperature.

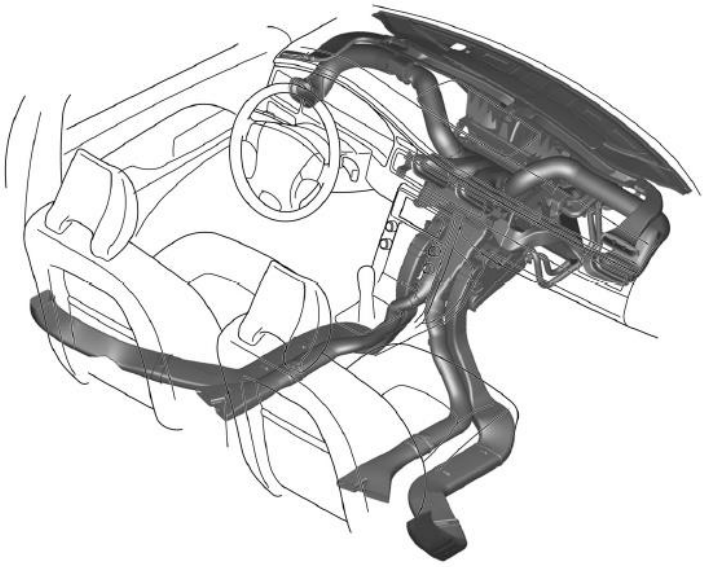

Figure 11. Air distribution and ducts of HVAC system. (Nielsen, F. 2016)

2.5 Passenger Compartment (Cabin)

Passengers compartment in this report considered as the cabin where provides housing and maintain desired air conditioning for passengers. In cold climate cabin requires heating while in warm climate ambient air needs to be cooled. The main thermal components of cabin are categorized to metal, windows and air based on their materials.

2.5.1 Metallic Boundaries

Doors, floor and roof are well insulated. Each part is made from three layers: interior, insulation and body part.

2.5.2 Windows and Windshield

Two functions of glasses are thermal insulation and visual contact with the outside environment.

2.5.3 Air Trapped Inside the Cabin

Air inside the cabin is also considered as a part of system in this thesis. The purpose is to facilitate the definition of heat transfer among the key components.
Detailed specification of components is not presented in this report due to confidential data protection policy at NEVS.

3 THEORY

Theories and equations presented in this chapter provide the basis of calculations embedded in GT-Suite and Star-CCM+ programs. The results of these calculations are provided in chapters 5 and 7 of this report.

3.1 Fluid Dynamics

The continuity equation (1) momentum equation (Navier-Stokes) (2) and the equation of energy conservation (5) govern the motion and heat transfer of a Newtonian viscous fluid. The continuity equation

$$\frac{\partial \rho}{\partial t} + \frac{\partial}{\partial x_i}(\rho v_i) = 0 \tag{1}$$

ρ $Density$ $[kg/m^3]$

v_i $Velocity$ [m/s]

t $Time\ coordinate$ $[s]$

x_i $Spatial\ coordinate$ $[m]$

Equation (1) is obtained from the conservation of mass and describes the rate of mass change in a fluid system is equal to summation of net mass flow in the fluid system. The Navier-Stokes equation is derived from the momentum equation:

$$\frac{\partial}{\partial t}(\rho v_i) + \frac{\partial}{\partial x_j}(\rho v_i v_j) = -\frac{\partial p}{\partial x_i} + \frac{\partial \tau_{ji}}{\partial x_j} + \rho f_i \tag{2}$$

$$\sigma_{ij} = -p\delta_{ij} + \tau_{ij} \tag{3}$$

$$\tau_{ij} = \mu\left(\frac{\partial v_i}{\partial x_j} + \frac{\partial v_j}{\partial x_i}\right) - \delta_{ij}\frac{2}{3}\mu\frac{\partial v_k}{\partial x_k} \tag{4}$$

σ_{ij} $Stress\ Tensor$

τ_{ij} $Viscous\ stress$

ρf_i $Body\ forces$

Equations (3) and (4) define the condition that the stresses of a fluid element can be decomposes into pressure and viscous stresses. The Navier-Stokes equation explains that the momentum change rate in a fluid equals the sum of forces on the element.
The equation for conservation of energy is:

$$\frac{\partial}{\partial t}(\rho e) + \frac{\partial}{\partial x_i}(\rho e v_i) = -p\frac{\partial v_i}{\partial x_i} + \Phi - \frac{\partial q_i}{\partial x_i} \quad (5)$$

e $Internal\ energy$

Φ $Viscous\ heating$

q_i $Heat\ flux$

Equation (5) denotes that the rate of charge in internal energy of fluid system is equal to the total energy in form of heat or work, added or removed from the system. (Ekh and Toll., 2016)

3.2 Turbulence modeling

Navier-Stokes equation is computationally expensive to be solved directly for complex geometries. An alternative method to decrease the required computational power is to assume the fluid is incompressible and take the average of continuity (1) and Navier-Stokes (5) equations in time into the Reynolds-Averaged Naviar-Stokes (RANS) equations

$$\frac{\partial \overline{v}_i}{\partial x_i} = 0 \quad (6)$$

$$\rho\frac{\partial \overline{v}_i \overline{v}_j}{\partial x_j} = -\frac{\partial \bar{p}}{\partial x_i} + \frac{\partial}{\partial x_j}\left(\mu\frac{\partial \overline{v}_i}{\partial x_j} - \rho\overline{v_i{}' v_j{}'}\right) \quad (7)$$

3.2.1 $k-\varepsilon$ Turbulence model

The most common used turbulence modelling method in CFD is $k-\varepsilon$. It is based on Boussinesq assumptions which defines that the Reynolds stresses, $\overline{v_i{}' v_j{}'}$, can be averaged similar to the viscous stresses by use of turbulent viscosity, v_t (Versteeg and Malalasekera, 2007). The equation will be

$$\overline{v_i{'}v_j{'}} = -v_t\left(\frac{\partial \overline{v_i}}{\partial x_j} + \frac{\partial \overline{v_i}}{\partial x_i}\right) + \frac{1}{3}\delta_{ij}\overline{v_k{'}v_k{'}} = -v_t\left(\frac{\partial \overline{v_i}}{\partial x_j} + \frac{\partial \overline{v_j}}{\partial x_i}\right) + \frac{2}{3}\delta_{ij}k \quad (8)$$

Through dimensional analysis a definition for the turbulent viscosity is derived.

$$v_t = c_\mu l v = c_\mu k^{0.5}\frac{k^{1.5}}{\varepsilon} = c_\mu \frac{k^2}{\varepsilon} \quad (9)$$

Where;

l $Turbulent\ length\ scale$

v $Turbulent\ velocity\ scale$

k $Kinetic\ energy$

ε $Dissipation\ rate$

The outcome of $k-\varepsilon$ turbulence model is reducing the six unknown Reynolds stresses into two unknowns of the turbulent kinetic energy(k) and the turbulent dissipation rate(ε).

3.3 Modes of Heat Transfer

The basic principle regarding heat transfer is the first law of thermodynamic. It states that in an isolated system total amount of energy remain constant. The energy balance for the first law of thermodynamic is:

$$m_{sys}C_p\frac{\partial T}{\partial t} = \dot{Q}_{convection} + \dot{Q}_{radiation} \quad (10)$$

m_{sys} $Mass\ of\ system$

C_p $Specific\ heat\ capacity$

$\dot{Q}$ $Heat\ transfer\ rate\ [W]$

Heat transfer has three modes: convection, conduction and radiation. Figure 12 shows the modes of heat transfer. The basic rate equations of each mode are depicted in table 3 (Vepsäläinen, 2012).

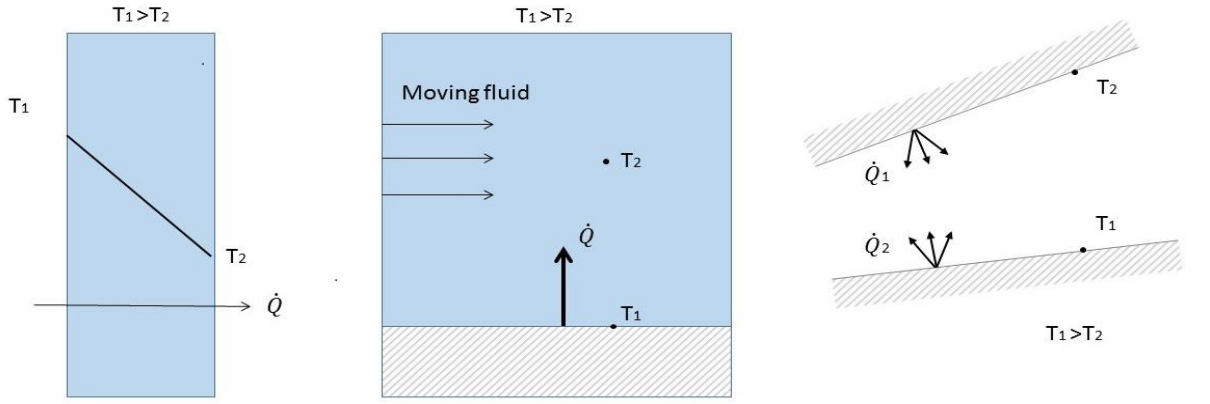

Thermal conduction in a solid material or a static fluid

Thermal conduction from a surface to a moving fluid (convection)

Heat transfer by thermal radiation from one surface to another

Figure 12. Heat transfer modes.

Table 3. Basic equation for heat transfer modes. (Vepsäläinen, 2012)

Conduction	Convection	Radiation
Heat transfer across medium	Heat transfer between solid surface and moving fluid	Heat transfer in mode of electromagnetic wave emission
$\dot{Q}_{cond} = -kA\,\frac{dT}{dx}$	$\dot{Q}_{conv} = HTC_{conv} \cdot A(T_S - T_\infty)$	$\dot{Q} = \varepsilon A\sigma(T_S^4 - T_\infty^4)$

3.4 Thermal Conductivity

Thermal conductivity is accounted as heat transfer in parts of a single body which have different temperatures. The particles with higher energy transfer it to the particles with less energy by direct contact. This mode of heat transfer is concerned more inside solid materials. Fourier's law is the main formula for conduction. It states that the conduction heat flux is related to the temperature gradient. (Vepsäläinen, 2012)

3.4.1 Fourier's Law

Fourier's law for one directional heat conduction states the relation of conductive heat transfer and temperature gradient:

$$\dot{Q}_{cond} = -kA\,\frac{dT}{dx} \tag{11}$$

$\dot{Q}_{cond}$ $Heat\ transfer\ rate\ [W]$
k $Thermal\ conductivity\ [W/mK]$
A $Area\ [m^2]$
dT/dx $Thermal\ gradient\ [K/m]$

In equation (11), thermal conductivity, k, depends on both material and temperature. The area, A, is perpendicular to the direct of heat transfer. Thermal gradient, dT/dx, is in the spatial direction orthogonal to the area.

Hoses and pipes have cylinder shapes. Conduction heat transfer of a cylinder body can be described by conduction resistance (R_{cond}):

$$q = \frac{(T_1 - T_2)}{R_{cond}} = Sk\ (T_1 - T_2) \tag{12}$$

$$q = \frac{2k\pi L}{\ln {}^{r_1}/_{r_2}}\ (T_1 - T_2) \tag{13}$$

R_{cond} $Thermal\ conduction\ resistance\ [\frac{mK}{W}]$
S $Shape\ factor$
k $Conductive\ heat\ transfer\ constant\ [W/mK]$

3.5 Convective Heat Transfer

Heat transfer between a static surface and a moving fluid is convection. Additionally, convection classifies to free convection and forced convection.
At free convection temperature gradient causes density difference and flow is induced by gravity force. In forced convection external pressure difference establishes the flow. (Vepsäläinen, 2012)

3.5.1 Newton's Law

Newton's law for cooling describes convective heat transfer:

$$\dot{Q}_{conv} = HTC_{conv} \cdot A(T_S - T_\infty) \quad (14)$$

HTC_{conv} $Convective\ heat\ transfer\ coeficient\ [W/Km^2]$

A $Area\ [m^2]$

T_S $Temperature\ of\ surface\ [K]$

T_∞ $Temperature\ of\ fluid\ [K]$

Convective heat transfer coefficient (HTC_{conv}) is function of surface geometry, configuration of flow motion, properties of fluid and ram air velocity. In this thesis, HTC_{conv} is determined based results of 3D simulation of entire vehicle body (Vepsäläinen, 2012).

3.6 Thermal Radiation

Thermal radiation is outcome of electromagnetic waves exchange between two matters at nonzero temperature with different temperatures. It happens even in absence of intervening medium. Although radiation is volumetric phenomenon, it is mostly regarded as heat transfer between surfaces.

3.6.1 Stefan-Boltzmann Law

Heat emission of a surface is given by Stefan-Boltzmann law:

$$\dot{Q} = \varepsilon A \sigma (T_S^4 - T_\infty^4) \quad (15)$$

$\dot{Q}$ $Heat\ transfer\ rate\ [W]$

ε $Gray\ surface\ emissivity$ [-]

A $Surface\ area\ [m^2]$

σ $Stefan - Boltzmann\ constant\ [W/m^2K^4]$

T_S $Absolute\ temperature\ of\ surface[K]$

T_∞ $Fluid\ temperature[K]$

In figure 12 above, the temperature T2 is less than T1, thus, the heat transfer is in the direction of the temperature T2. In terms of thermal radiation, both surfaces radiate and proportionally absorb thermal energy and the heat flux of surface 1 is more than the other. (Vepsäläinen, 2012)

The amount of received solar radiation on each specific surface is dependent on direction of surfaces. Equation (16) below defines the relation of intensity with the rate of emitted radiation energy and the normal area.

$$I_e(\theta,\phi) = \frac{d\dot{Q}_e}{dA\cos\theta\,.\,d\Omega} = \frac{d\dot{Q}_e}{dA\cos\theta\sin\theta.\,d\theta d\phi} \tag{16}$$

$I_e(\theta,\phi)$ $\quad Radiation\ intensity\ [W/m^2 sr]$

$d\dot{Q}_e$ $\quad Energy\ emission\ rate\ [W]$

The $dA\cos\theta$ term represents the projection of dA area at an angle of θ from the surface normal. ϕ here states the direction of surface normal vector. $d\Omega$ is the solid angle on the sphere surface and which is the fraction of sphere surface area by the square of the radius. The SI unit of solid angle is steradian [sr] (Lidar, 2018).

$$d\Omega = \frac{dS}{r^2} = \sin\theta.\,d\theta d\phi \tag{17}$$

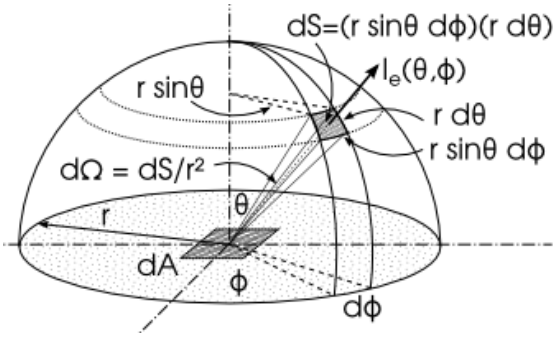

Figure 13. Geometries for calculating radiation intensity. (Lidar, 2018)

3.6.2 Surface to Surface radiation (S2S)

In this thesis the effect of solar radiation on the cabin is investigated based on S2S radiation method. Radiation is mostly studied in solids as surface to surface and is dependent on the

orientation of the surfaces. To consider how they face each other, view factors are commonly used. The view factor $F_{i\to j}$ addresses the fraction of radiation which leaves the surface *i* and directly received at surface *j*. The first step to find the view factor is to formulate the total rate of radiation which leaves the surface $dA_1$and receives and surface dA_2 ($\dot{Q}_{dA_1\to dA_2}$). The geometry of surfaces is shown in figure 14 below.

$$\dot{Q}_{dA_1\to dA_2} = I_1 dA_1 \cos\theta_1 \, d\Omega_1 = I_1 dA_1 \cos\theta_1 \frac{dA_2 \cos\theta_2}{L^2} \tag{18}$$

where;

I_1 $Total\ intensity\ leaving\ dA_1\ [W/m^2 sr]$

θ_1 $The\ angle\ between\ surface\ normal\ of\ dA_1\ and\ connecting\ line$

$d\Omega_1$ $Solid\ angle\ when\ viewed\ from\ dA_2\ [sr]$

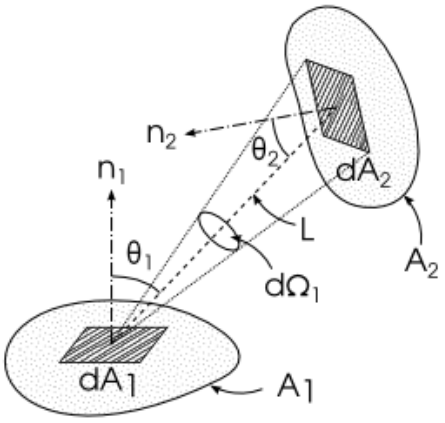

Figure 14. Geometry of surfaces. (Lidar, 2018)

The total radiation which leaves the surface dA_1 is calculated in equation (19) below

$$\dot{Q}_{dA_1} = \pi I_1 dA_1 \tag{19}$$

Thus, the view factor is

$$dF_{dA_1\to dA_2} = \frac{\dot{Q}_{dA_1\to dA_2}}{\dot{Q}_{dA_1}} = \frac{\cos\theta_1 \cos\theta_2}{\pi L^2} dA_2 \tag{20}$$

The radiation rate from surface A_1 to surface A_2 is obtained by integrating the radiation rate from dA_1 to dA_2

$$\dot{Q}_{A_1 \to A_2} = \int_{A_2} \dot{Q}_{A_1 \to dA_2} = \int_{A_2} \int_{A_1} \frac{I_1 \cos\theta_1 \cos\theta_2}{L^2} dA_1 dA_2 \quad (21)$$

Then the view factor for the finite surfaces of A_1 and A_2 is then calculated

$$F_{A_1 \to A_2} = \frac{\dot{Q}_{A_1 \to A_2}}{\dot{Q}_{A_1}} = \frac{1}{A_1} \int_{A_2} \int_{A_1} \frac{\cos\theta_1 \cos\theta_2}{\pi L^2} dA_1 dA_2 \quad (22)$$

The other important terms in radiation are transmissivity and reflectivity. The theory for these factors is not described in this report, however it is available on (Siegel, Howell and Mengüç, 2011).

3.7 Energy Balance

The first law of thermodynamics represents the conservation of energy, and it explains that in a close system, energy is neither eliminated nor created. Net energy is constant in a closed system. (Nielsen, F. 2016)

$$\frac{dE_{C.V.}}{dt} = \dot{Q}_{C.V.} + \dot{W}_{C.V.} + \sum \dot{m}_i (h_i + \frac{1}{2} {V_i}^2 + gZ_i) - \sum \dot{m}_e (h_e + \frac{1}{2} {V_e}^2 + gZ_e) \quad (23)$$

Where;

$E_{C.V.}$: energy of control volume [J]

$\dot{Q}_{C.V.}$: heat rate to the control volume [W]

$\dot{W}_{C.V.}$: work rate on the control volume [W]

$\dot{m}_i$: mass flow [kg/s]

h: enthalpy [J/kg]

V: velocity [m/s]

gZ: potential energy [J]

The subscription i and e denotes incoming and outgoing flow.

For the simplicity of calculation, it is assumed that changes in kinetic or potential energy are negligible. The equation (23) is then written as:

$$\dot{Q}_{C.V.} + \dot{W}_{C.V.} + \dot{m}_{osa}h_{osa} + \dot{m}_{rec}h_{rec} - \dot{m}_{pass.comp}h_{pass.comp} = 0 \quad (24)$$

3.7.1 Cabin Heat Transfer

In warm climate condition, heat enters the cabin through cabin boundaries and solar radiation. The task of cooling system is to take out the extra heat via evaporator of the HVAC unit. Extra heat exists the cabin from outlet port and wastes thermal energy. Figure 15 below demonstrates the energy balance inside the cabin.

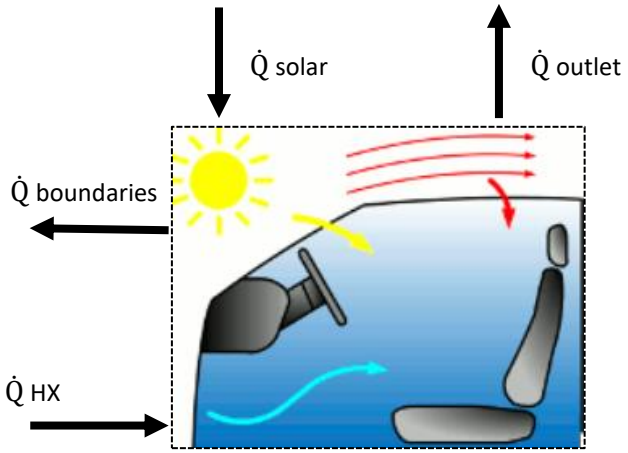

Figure 15. Thermal energy balance inside the cabin.

Equation 25 below formulates the energy balance of cabin.

$$\dot{Q}_{sun,passengers} + \dot{Q}_{intake\ via\ boundaries} + \dot{Q}_{inlet\ air} - \dot{Q}_{outlet\ air} = 0 \quad (25)$$

$$\dot{Q}_{sun,passengers} + \dot{Q}_{intake\ via\ boundaries} = \dot{m}_{out} * c_p * T_{out} - \dot{m}_{in} * c_p * T_{in} \quad (26)$$

$$\dot{m}_{in} = \dot{m}_{out} = \dot{m} \quad (27)$$

$$\dot{Q}_{sun,passengers} + \dot{Q}_{intake\ via\ boundaries} = \dot{m} * c_p * (T_{out} - T_{in}) \quad (28)$$

Heat loss of air leaving the cabin in cooling mode is regarded as the difference between the energy rate of evaporator and heat removed by the airflow leaving the cabin.

$$\dot{Q}_{loss,outlet} = \dot{Q}_{EVAP} - \dot{Q}_{heat\ removal,air} \quad (29)$$

3.7.2 RESS Heat Transfer

The sources of thermal energy in battery cooling/heating system are:

- Thermal energy of coolant
- Heat generation in the battery modules (Self-heating)
- Heat loss via top and bottom covers

Heat transfer in the RESS box is studied in two modes of heating and cooling.

Figure 16. RESS system heating mode (left) and cooling mode (right). (Chevrolet, 2018)

In heating mode, the average temperature of battery modules is less than 25℃ which is minimum functional temperature. Warm coolant flow and self-heating capability of battery cells increase the internal temperature of RESS box. Contrarily RESS box loses heat convective heat transfer to the ambient air.

$$\dot{Q}_{loss,TOTAL} = \dot{Q}_{Coolant} + \dot{Q}_{Self\ heating} = \dot{Q}_{loss\ via\ boundaries} \quad (30)$$

In cooling mode, cold coolant flow takes out the excess heat gained from battery self-heating and ambient air. Equation (15) defines the energy balance in RESS box for cooling mode.

$$\dot{Q}_{loss,TOTAL} = \dot{Q}_{Coolant} = \dot{Q}_{Self\ heating} + \dot{Q}_{intake\ \ via\ boundaries} \quad (31)$$

3.7.3 Heat transfer in Propulsion Loop

In heat transfer of propulsion loop, it is assumed that the total amount of heat produced in the propulsion loop is taken out to the coolant and dissipates to ambient air through the radiator (heat exchanger). Thus, the total rate of heat release through the heat exchanger is considered as the heat loss of the propulsion loop.

3.8 Finite volume method

Finite volume method is the most common approach in solving computational fluids dynamics problems. Its fundamental approach is to divide the domain into a grid of finite control volumes and apply the governing equations to the grid by discretization. Practically, the first step in dividing the domain is to prepare the geometry and fix the errors and then meshing the surfaces and volumes to finite volume grid.

3.8.1 Discretizational method

A transport equation for the general property ∅ (described in figure 17) is formulated as

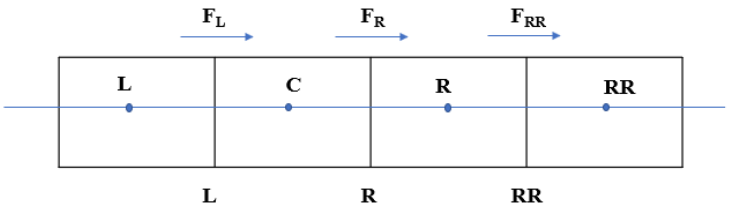

Figure 17. One dimensional grid with, center point C, Left point L, Right point R, and Right of Right (RR). Faces L, C and R are between the control volumes and grid flux at each face is F_L, F_R, F_{RR}.

$$\frac{\partial(\rho\emptyset_i)}{\partial t} + \frac{\partial}{\partial x_j}(\rho\emptyset_i u_j) = \frac{\partial}{\partial x_j}\left(\Gamma\frac{\partial\emptyset_j}{\partial x_i}\right) + S_\emptyset \qquad (32)$$

Equation (32) is the general equation in finite volume method for discretizing the governing equations. It defines the rate of change in parameter ∅ plus the flowrate of ∅ out of fluid is

equal to the rate of change in ∅ from diffusion plus the rate of change in ∅ related to external sources. While equation (32) describes the 1D discretizing, there is also need for 3D discretizing for use in Star-CCM+ program. By integrating equation (32) over a 3D control volume and use of Gauss's divergence theorem the equation (33) is acquired.

$$\frac{\partial}{\partial t}\left(\int_{CV} \rho\phi dV\right) + \int_{A} n_j.\left(\rho\phi u_j\right)dA = \int_{A} n_j.\left(\Gamma\frac{\partial \emptyset}{\partial x_j}\right)dA + \int_{CV} S_{\emptyset}dV \qquad (33)$$

In equation (33), *n* represents the surface normal vector and the product of second and third terms are vectors in the direction of surface normal. Therefore, the result of these two terms is flux of ϕ through convection and diffusion respectively. The equation (33) can be applied to a three-dimensional geometry by approximating the integrals to the flux of a small control volume. (Versteeg and Malalasekera, 2007)

3.8.1.1 Discretizational Schemes

The fluxes between the control volumes exist at the corresponding faces, however, the value of variable ϕ is stored at the center node of the control volume. Thus, the value for the fluxes are approximated based on the center node of the adjacent cell. The principle of this approximation method is named discretizational scheme. The fluxes are the main points to calculate the values on new center node, so a new value is assigned at the center node of a specific control volume. First order upwind scheme and second order upwind scheme are the two most common discretizational schemes.

4 1 D SIMULATION OF TM SYSTEM IN GT-SUITE

This chapter introduces the one-dimensional models of EV's thermal management system for both cooling and heating modes. The models are created in GT-ISE V2018 program. The results of simulation in each mode is presented in the Chapter 5.

4.1 Modelling and Calculations in GT-Suite

GT-Suite is simulation tool applicable for broad range of applications and industries. It comprises variety of multi-physics platforms for building models of general systems using many fundamental libraries such as: Flow, Acoustics, thermal, mechanical, electric, chemistry, etc. Flow, mechanical and thermal libraries are used in this study to perform 1D simulation for thermal system of EV.

4.1.1 Basics of Modeling in GT-Suite

GT-Suite program has object oriented graphical interface. In order to build a model, one needs to select appropriate template from the library and fill in required attributes to form a component object. Then by dragging and dropping the parts into a plain model and connecting proper ports, the entire model is built.

The hierarchy of components is: template, object, part. Each template may include several objects and each object can contain several parts. The attributes of different objects in a template may be similar or distinct.

Using one template it is possible to create many objects of one kind with different attributes. And one object can be used to create as many parts as needed. Table 4 below shows representation of selected parts in the GT-Suite platform.

Table 4. Description of selected parts in GT-Suite.

No.	Template name	Application	Symbol
1	Compressor	Refrigerant Compressor	
2	Heat exchanger	Radiators, HVAC heat exchangers, chiller	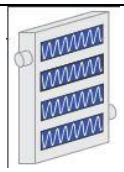
3	Fan	CRFM (Condenser/Radiator/Fan Modules), blower	
4	End Environment inlet	HVAC and radiators air inlet	
5	Heat addition	E-motor, battery modules, electric heater	
6	Liquid pump	Coolant pumps	
7	Pipe	Pipes and hoses	
8	Pressure loss connector	HVAC pressure loss	
9	Orifice connector	Pipes and components connection	
10	Actuator connector	Contol system	
11	Sensor connector	Control system	

The corresponding attributes and information for the components are filled based on the data provided by the supplier of the components. The next task after defining the parts is to

connect them using proper links and connectors. Example of some connection objects are listed in rows 7-11 of table 4.

There are many details regarding modeling in GT-ISE interface which are not in scope of this study. More information and instructions for this program can be found at GT-ISE tutorials database (Gamma Technologies, 2016)

4.2 Methods

In this thesis 6 uses cases are defined to include every possible condition of thermal system (table 5). Heating mode is defined as three use cases where ambient temperature is -10℃ while cooling mode is when ambient temperature is +30℃. These values for ambient temperature are assumed based on interview with relevant professionals at NEVS. The simulation is done in steady-state mode.

Table 5. Defined use cases of the thermal system.

Ambient temperature / **Vehicle speed**	**-10**℃ (Heating mode)	**+30**℃ (Cooling mode)
40 [kph]	Case 1	Case 4
80 [kph]	Case 2	Case 5
120 [kph]	Case 3	Case 6

4.2.1 Cooling mode

In the cooling mode, the objective of thermal management system is to absorb excessive heat from the components and release it to the ambient air. Components of the cooling mode have been described in the table 4. Figure 18 demonstrates the overall layout of EV's thermal system in GT-Suite.

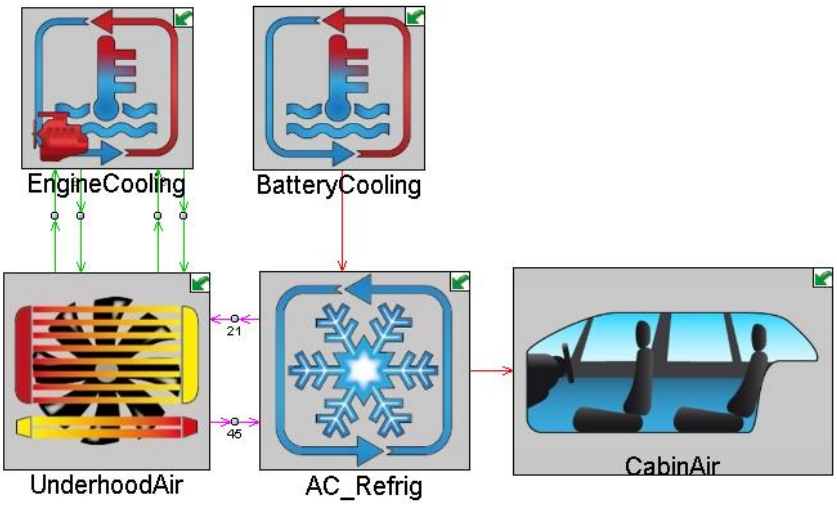

Figure 18. Overall 1D model of EV's thermal system in GT-Suite for cooling mode.

4.2.1.1 Boundary conditions

The values used to run the system in cooling mode are listed in table 6. Initial values for the system are obtained based on discussion with experts in HVAC department of NEVS and after some iterations the final values are reached. The final values from Table 6 are sensible values and do not necessarily apply to the NEVS system.

Table 6. Boundary conditions for cooling mode.

Vehicle Speed	**kph**	**40**	**80**	**120**
Cabin Air Recirculation	%	90	90	90
HVAC Volumetric flow rate	L/s	70	70	70
Compressor speed	%	83	84	100
RESS Coolant pump speed	%	100	100	100
Solar Radiation	W/m^2	1006	1006	1006
Relative Humidity	-	0,4	0,4	0,4

The properties of cabin boundaries such as materials, thickness and area are defined according to the data driven from interior design experts at NEVS. The value of view factor (see section 3.6.2) for each boundary of cabin is assumed to be the default value of GT-Suite cabin template and are in range of [0.5-0.9] for different boundaries of cabin.

4.2.2 Heating mode

In the heating mode, the objective of thermal management system is to supply required heat for each component. Figure 16 demonstrates the overall layout of EV's thermal system in GT-Suite for heating mode.

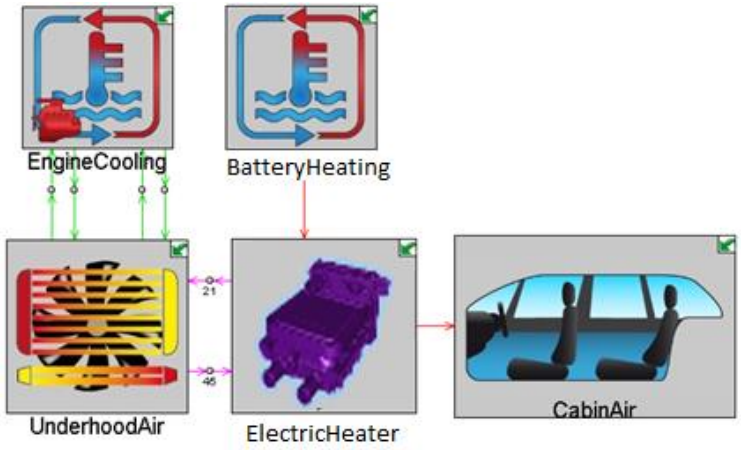

Figure 19. Overall 1D model of EV's thermal system in GT-Suite for heating mode.

4.2.2.1 Boundary conditions

The values used to run the system in heating mode are listed in table 7. Initial values for the system are obtained based on discussion with experts in HVAC department of NEVS and after some iterations, the final values are reached. The final values from Table 7 are sensible values and do not necessarily apply to the NEVS system.

Table 7. Boundary conditions for heating mode.

Vehicle Speed	**kph**	**40**	**80**	**120**
Cabin Air Recirculation	%	25	25	25
HVAC Volumetric flow rate	L/s	54	54	54
Heater Power	%	100	100	90
RESS Coolant pump speed	%	100	100	100

Cabin Coolant pump speed	%	100	100	100
Solar Radiation	W/m^2	5	5	5
RESS modules heat rate	%	8	27	100

5 RESULTS OF 1D SIMULATION IN GT-SUITE

This chapter describes the model built for simulating the system and demonstrate the corresponding results. Both cooling and heating mode are simulated in GT-Suite program and the results of heat transfer for each subsystem is discussed in this chapter.

5.1 Cooling Mode

Section 5.1 presents the results for 1D simulation of thermal system in cooling mode. Results are categorized in three main parts of cabin, propulsion and battery thermal system as well as heat loss from hoses and pipes.

5.1.1 Cabin

Based on equation (12) the sources of heat in cabin air volume are direct solar radiation and convective heat transfer. On the other hand, evaporator removes the heat from supplied air to the cabin. The air leaving the cabin also removes some extend of cooled air.
As mentioned in table 4 numerous parameters (such as compressor speed, changes external HTC, RESS temperature and required power for the chiller) effect the thermal system. After some iterations, the best match for these parameters obtained to supply the average cabin temperature around 24 ℃. Figure 20 shows the ratio of energy sources in the cabin volume. Transmitted solar radiation has the most contribution which is about 80% of total transmitted heat.

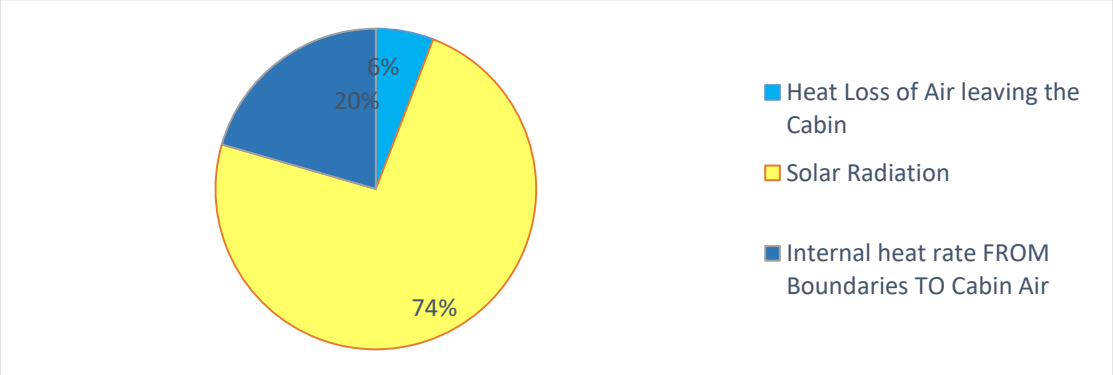

Figure 20. Sources of heat gain in EV's cabin for cooling mode.

Beside solar radiation, cabin boundaries (windows, roof, floor and door) is the second source of heat loss of the cabin in cooling mode. Figure 21 depicts the heat loss through each part of cabin boundaries. Front windshield and roof have the highest contribution to the cabin heat intake, following by side and rear windows.

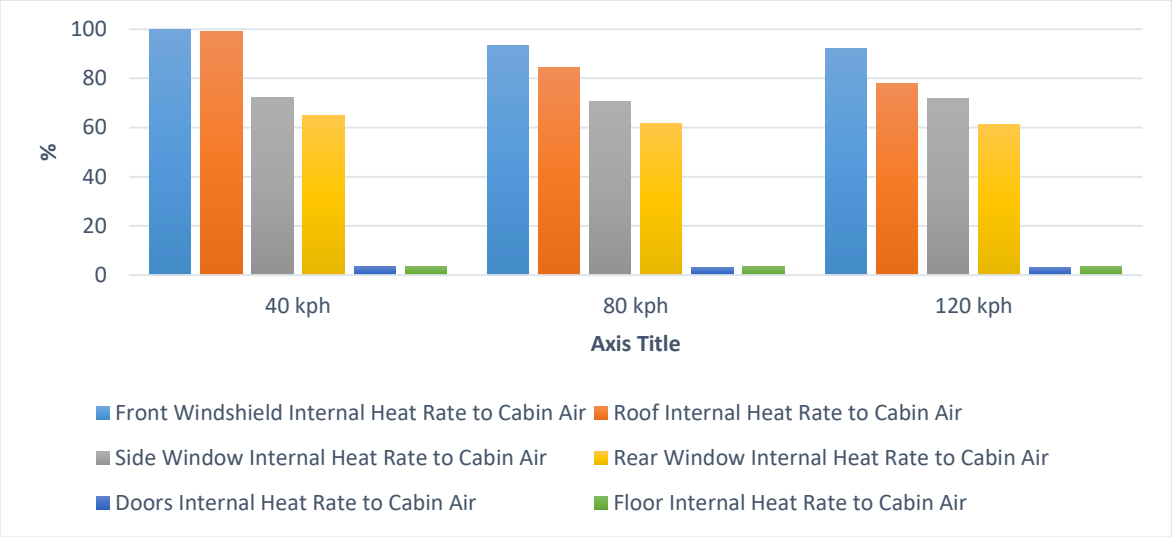

Figure 21. Heat gain via different boundaries of EV's cabin in cooling mode.

5.1.2 Battery

Maintaining the RESS temperature in cooling mode is more challenging than other sub-systems due to lack of control. The only control parameter for the cooling system in refrigerant loop is the compressor speed.

As mentioned in section 2.3.1 the average battery temperature should remain in range of 25 to 35 °C. Thus, by applying the boundary conditions listed in table 6 heat loss in RESS box is calculated. Detailed results of heat rate in RESS for cooling mode are listed in the figure 22. The ambient temperature in this mode is assumed to be 30℃ while the average module temperature in the following cases is obtained as 25, 26 and 31℃ corresponding. Therefore, the heat rate from RESS to ambient air is positive in two first cases and negative in the third.

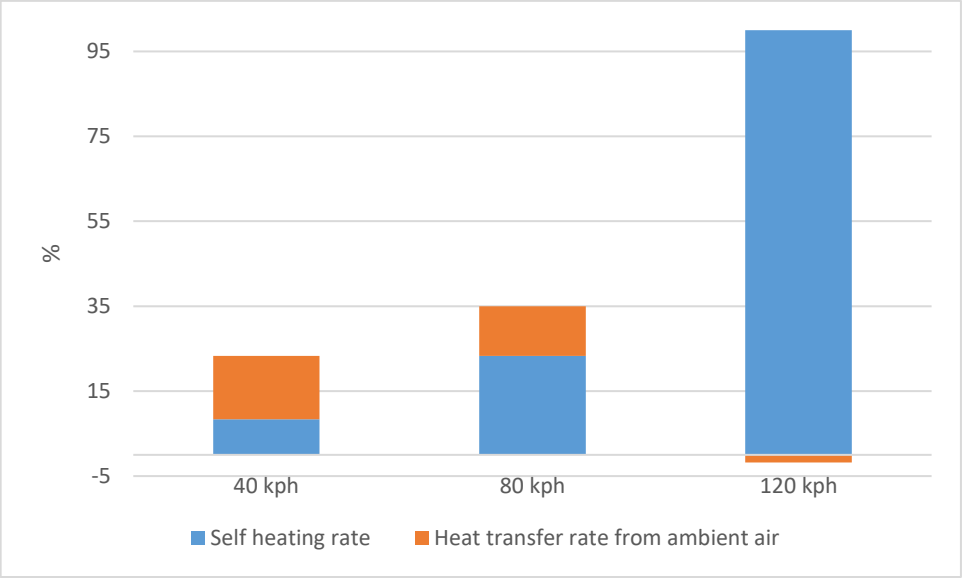

Figure 22. Heat loss in RESS box for cooling mode.

5.1.3 Powertrain Loop

In propulsion loop, it is assumed that all the generated heat is dissipated through the radiator. The heat rate of the powertrain radiator is demonstrated in the figure 23 below.

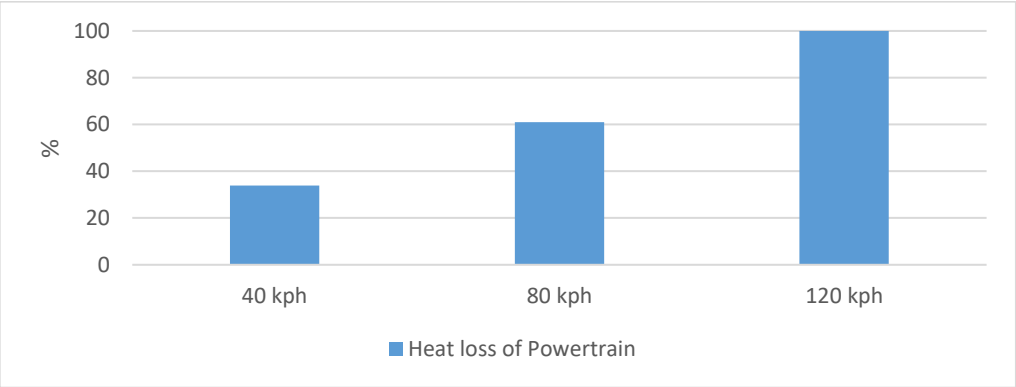

Figure 23. Heat loss in propulsion loop for cooling mode.

5.1.4 Pipes and Hoses

Pipes and hoses have the least heat loss comparing with other components of thermal system in cooling mode. The reason is low temperature difference between the coolant/refrigerant and ambient temperature. The values of heat loss of pipes and hoses for the three use cases is demonstrated in figure 24.

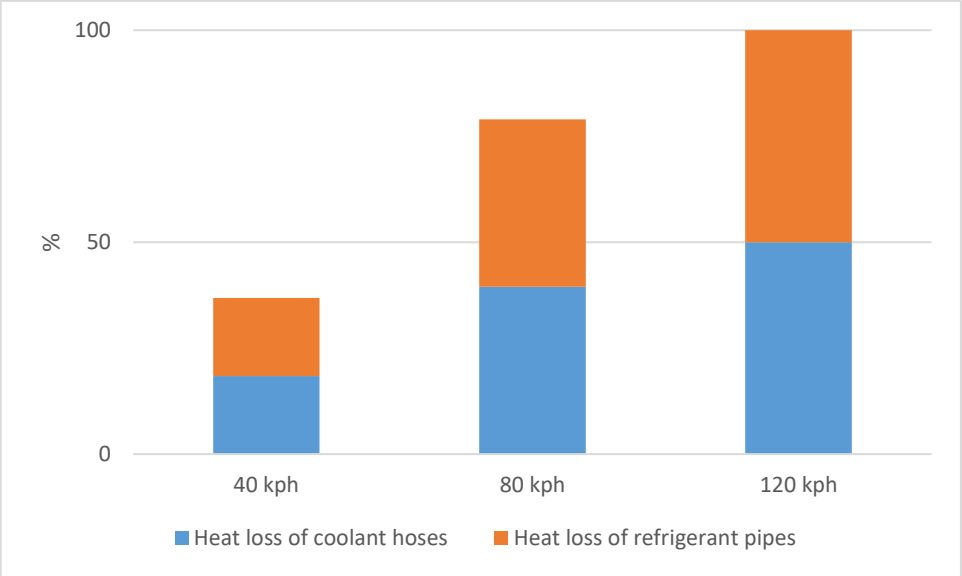

Figure 24. Heat loss in pipes and hoses for cooling mode.

5.2 Heating Mode

Section 5.2 presents the results for 1D simulation of thermal system in heating mode. Results are categorized in three main parts of cabin, propulsion and battery thermal system as well as heat loss from hoses.

5.2.1 Cabin

Figure 25 shows the ratio of energy sources in the cabin volume. As showed in table 4 numerous parameters effect the thermal system. 75% of the air in this mode is not recirculated and released to the ambient air to prevent the fog on the windows. After some iterations, the best match for these parameters obtained to supply the average cabin temperature of 24-25 ℃.

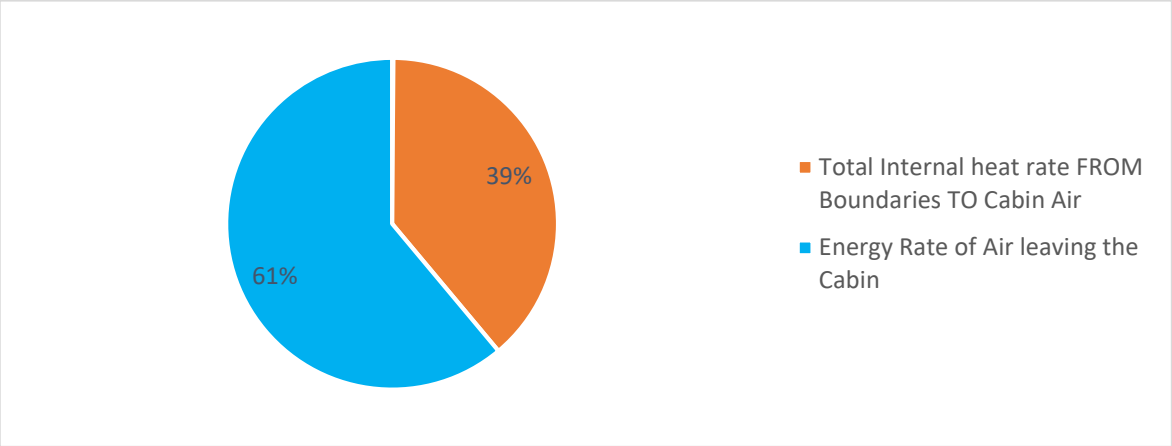

Figure 25. Sources of heat loss in EV's cabin for heating mode.

Figure 25 above shows that the power loss through the cabin boundaries in this mode is more than one kilowatt which is 39% of heat loss in cabin. Figure 26 demonstrates that most of the heat is leaving the cabin from windows. Front windshield, side and rear windows have the most heat loss among cabin boundaries respectively.

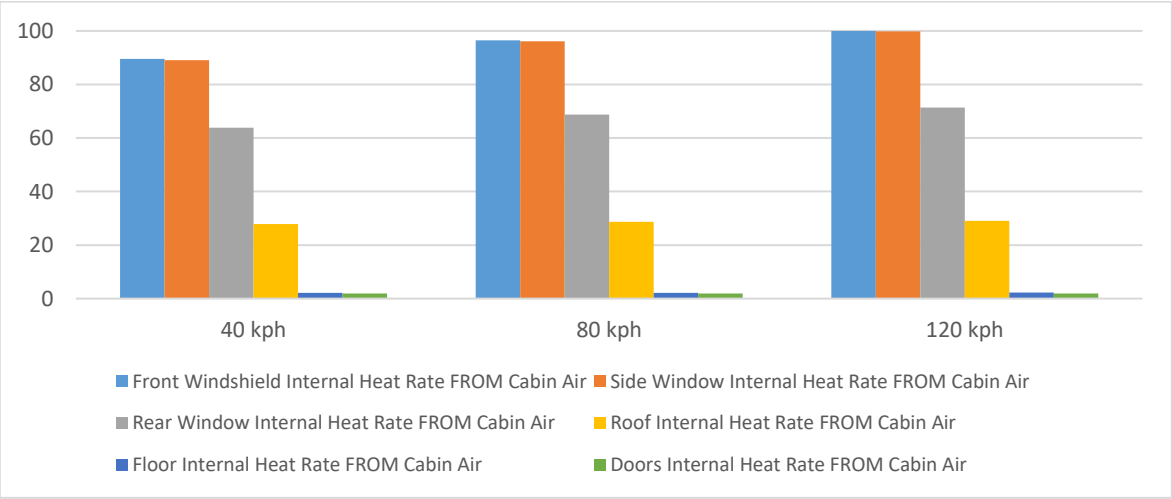

Figure 26. Heat loss via different boundaries of EV's cabin in heating mode.

5.2.2 Battery

In heating mode, electric heater produces heat and supplies heating circuits of both HVAC unit and RESS heat exchanger. Two sources of heat in the RESS heating loop are the coolant and self-heating of the battery modules. In the other hand, heat transfers to through the RESS

boundaries to the ambient air. Figure 27 below shows the results of RESS heating for three use cases.

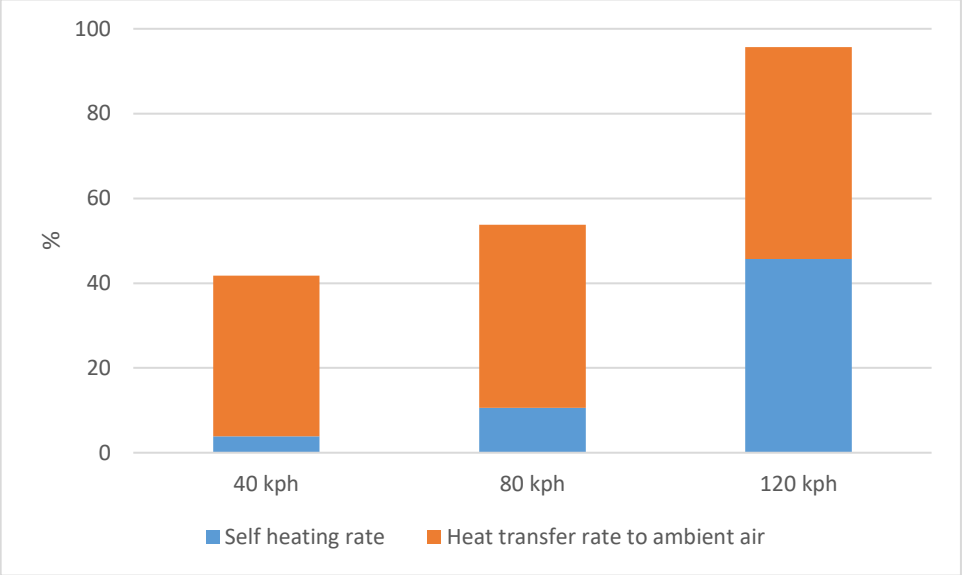

Figure 27. Heat loss in RESS box for heating mode.

5.2.3 Propulsion

In propulsion loop, it is assumed that all the generated heat is dissipated through the radiator. The heat rate of the powertrain radiator for three specified cases are demonstrated in the figure 28.

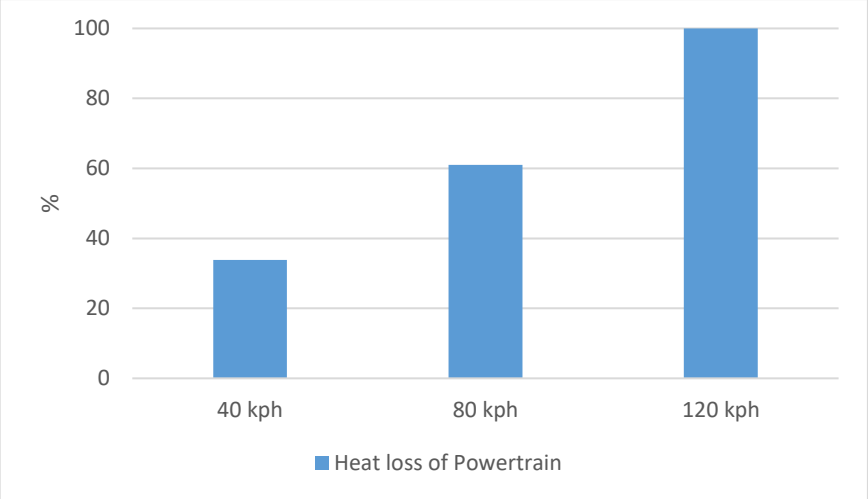

Figure 28. Heat loss in propulsion loop for heating mode.

5.2.4 Coolant Hoses

Figure 29 below shows the heat loss of coolant hoses in heating mode. Since the refrigerant pipes are not used in this mode, only the coolant hoses are monitored in this section. The temperature difference between coolant and ambient temperature is higher in this mode (~35℃), thus the convective heat loss is increased.

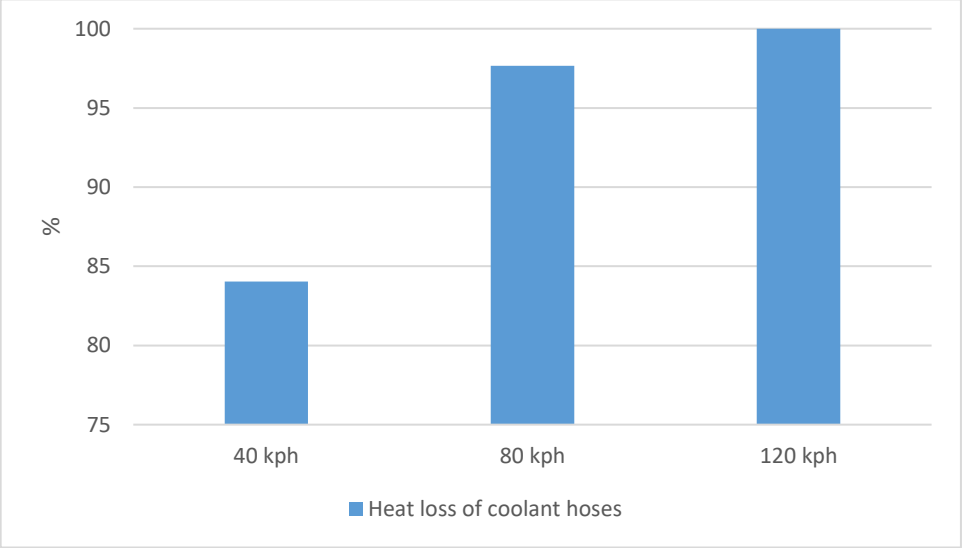

Figure 29. Heat loss from coolant hoses in heating mode.

6 3D SIMULATION OF VEHICLE'S CABIN IN STAR-CCM+

This chapter presents the 3D simulation of cabin air volume in Star-CCM+ from CD-Adapco. It is a powerful program in Computational Fluids Dynamics (CFD) calculations as well as solids from the early stage of CAD file preparation to post-processing the results.
The reason for performing 3D simulation is to investigate the effect of insulations on cabin boundaries with more accuracy than 1D simulation. In addition, 3D simulation provides possibility to study solar radiation inside the cabin in more details. Temperature distribution in the cabin air volume is the other parameter which effect the passengers' comfort and 3D simulation provides temperature at every points of cabin air.

6.1 Star-CCM+ Terminology

Each model in Star-CCM+ is called a *simulation*. All the required data is entered and the both pre and post process information are stored within a simulation file.

Region is the computational domain of the program. Each region is discretized according to finite volume method to perform the corresponding computations. Discretization process of regions is called *meshing*. Regions are surrounded by *boundaries* which can be isolated or common with two regions. The common boundaries can be joined with an interface allowing the interchange of energy, mass and momentum.

The geometrical representation of an object is called *part*. Parts are the input for meshing tools and the result of meshing will be stored in a region as described before. For the surfaces which are common between two parts the *contacts* are created (Lidar, 2018).

6.2 Problem definition

Since most of the thermal energy is transferred through the cabin glasses, two solutions regarding summer (+30 C) and winter (-10 C) conditions for average speed of 80 kph are presented. To investigate the performance of each solution, the baseline model and enhanced model are compared. In summer condition most of the heat enters the cabin via solar

radiation. Reducing the transmissivity of the glass causes less radiation to enter the cabin (figure 35). Solar radiation spectrum consists of three main spectral bands: UV (0.01-0.4 um), Visible (0.4-0.7 um), IR (0.7 to 1000 um). Figure 30 show the principle of solar reflection in glass.

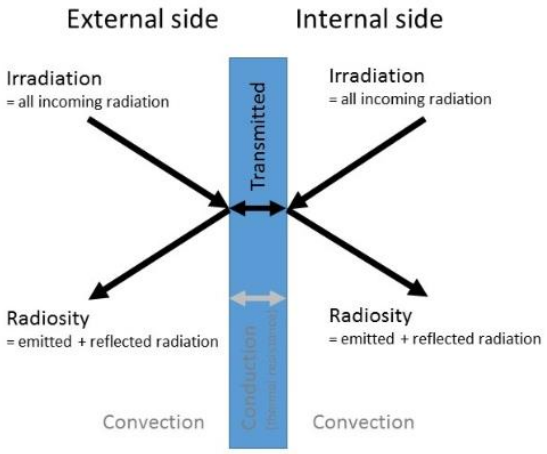

Figure 30. The reflection and refraction of solar radiation in vehicle's glass.

At mentioned in chapter 3 the most effective mode of heat transfer in absence of radiation is convection. In order to decrease the rate of heat loss in winter, the proposed solution is to define air barrier at the glass boundaries, by using double-pane glass. The air gap in between of two layers will decrease the heat loss due to lower value of HTC for trapped air.

6.3 Method

The initial step to build the 3D simulation setup is to prepare a CAD model for cabin and proposed glass solutions. Then by applying relevant physics and boundary conditions in both cooling and heating modes, the model is built and results are evaluated. Star-CCM+ v13.04 is used to run the 3D simulation.

6.3.1 CAD Preparation and Cleanup

The model used for 3D simulation is based on generic cabin air volume model. The first step to prepare the model for simulation is geometry cleaning. It includes correcting and

redesigning the intersecting and overlapping faces and surfaces therefore it will be more convenient to build the mesh also mesh quality is improved.

The volumes needed to be closed and manifold in Star-CCM+ prior to meshing and simulation. Thus, the surfaces should be checked for geometries errors such as free edges, pierced faces, non-manifold vertices and non-manifold edges. Figure 31 (a,b,c,d) shows the possible errors in the model geometry.

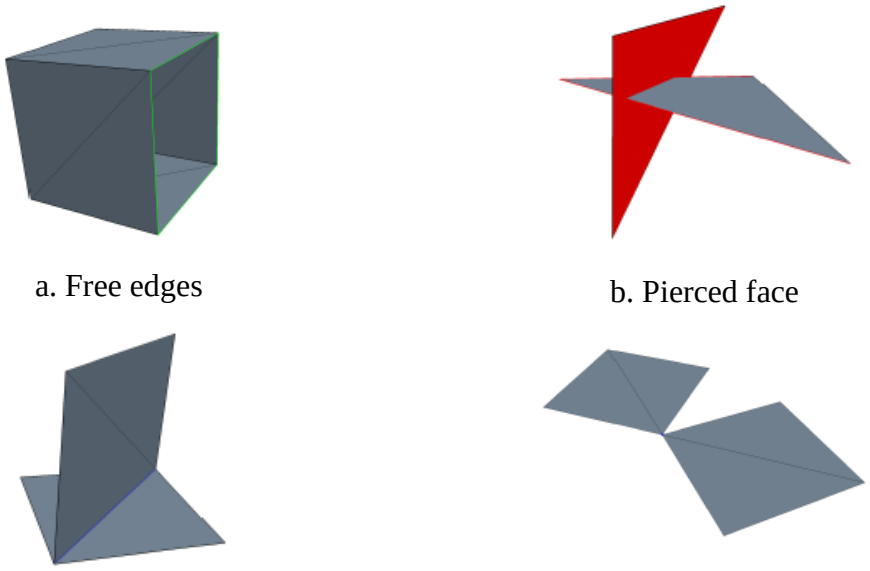

a. Free edges

b. Pierced face

c. Non-manifold edge

d. Non-manifold vertex

Figure 31. Errors in surface preparation in Star-CCM+.

Free edges are the ones which are only connected to one other face and a pierced face means a surface which intersects with another one. Non-manifold edges are the edges which are connected to more than two faces. A non-manifold vertex error occurs when the vertex is the only available connection of two faces. These errors can be fixed within Star-CCM+ or CAD program. CAD cleaning task is carried out using ANSA, 2017.

6.3.2 Meshing

In mesh generating process the domain is changed into a finite volume representation on which the governing equations are utilized. Mesh generation for a 3D model comprise a

surface mesh which captures the physical phenomena adjacent to the surface of geometry and a volume mesh to capture the flow inside the domain. Figure 33 shows the overall meshing of the generic cabin model.

6.3.2.1 Geometry of elements in volume mesh

Several cell shapes are available for performing volume mesh. Figure 32 below show the different available volume mesh geometries in most of CFD packages. Each of these mesh types have their specific properties. For detailed comparison please see Lidar, 2018.

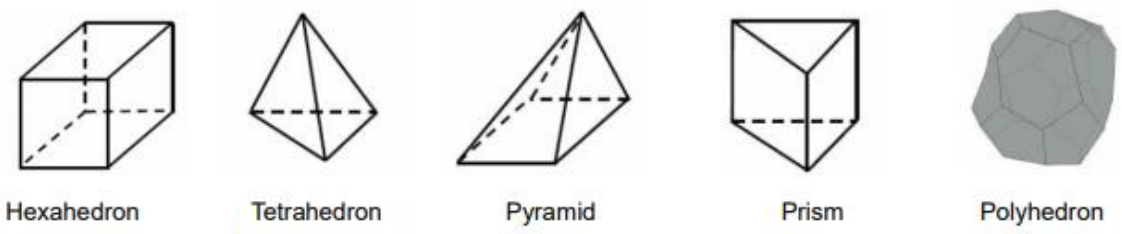

Figure 32. Options for structured volume mesh in Star-CCM+.

Polyhedral meshing is used for modelling the air volume inside the cabin due to simplicity and efficiency of model. Although, polyhedral mesh is not a good choice for regions with complex geometries or with thin dimensions specifically for a coarse mesh size. In these conditions thin mesher is activated for supporting polyhedral mesh. Prism mesher builds cells using polyhedral base and rectangular side shape. This mesh model is the most efficient for the cells adjacent to the boundary walls to capture the gradients of fluid parameters such as heat transfer and velocity.

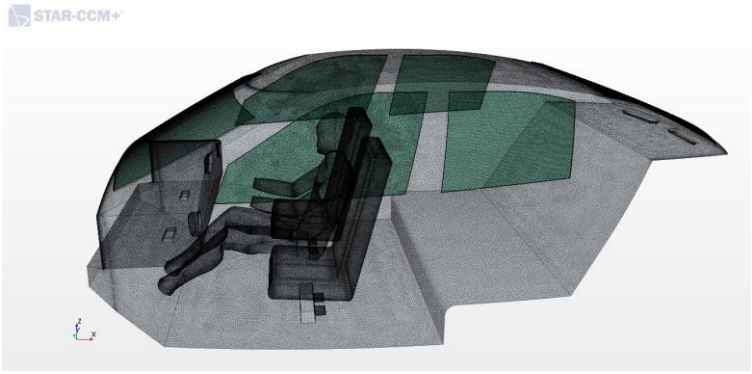

Figure 33. Mesh generation in Star-CCM+.

6.4 Physics Setup and Boundary Conditions

Based on material, 3D model can be divided to solid and gas parts. The air inside the cabin is considered as ideal gas and the material of solid part is glass. Table 8 below describes main physics setup for 3D simulation.

Table 8. Physics conditions.

Air	Radiation	Ideal gas	Turbulent k-ε	Buoyant (gravity)
Solid	Radiation	Glass	Constant density	

This section represents the boundary conditions for both cooling and heating modes. In order to assess the effect of proposed modifications in each mode, one baseline and one modified model is defined. The vehicle speed for 3D simulation is assumed to be 80 kph.

6.4.1 Cooling Mode

Cool air is supplied to the cabin volume through center, left and right vents to cool down the air inside the cabin. Baseline and modified cases are defined to investigate the effect of tinting glasses on the cabin air condition. Table 9 below shows the boundary conditions for cooling mode.

Table 9. Boundary conditions of air flow for cooling mode.

Boundary	**Boundary type**	**Physics value**	**Temperature**
Side vents	Volume flow	25 l/s	13 ℃
Center vent	Volume flow	50 l/s	13 ℃
Outlet	Pressure outlet	1 atm	13 ℃

In order to investigate the effect of changes in vehicles air conditioning, in modified case approximately the same average temperature in the cabin is obtained. To do so, in 8 iteration steps the temperature of inlet air is increased.

The position of sun in cooling mode is calculated by radiation calculator feature of Star-CCM+ for city of Trollhättan on 21st of June which is the longest day and shortest night in the northern hemisphere. Figure and table 34 below show the schematic of sun position against vehicle's cabin.

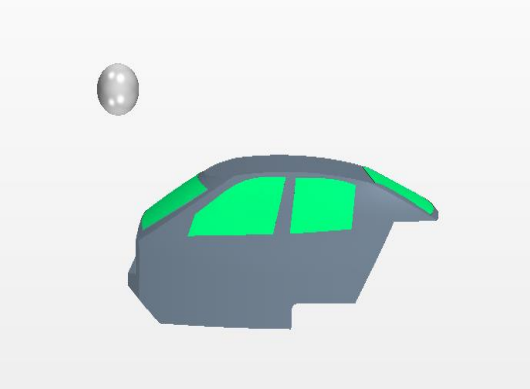

Solar properties	
City	Trollhättan, Sweden
Solar flux	1006 W/m2
Azimuth	3.095 rad
Altitude	0.848 rad

Figure 34. Schematic of sun position against vehicle's cabin.

Additional boundary conditions are defined for the glass boundaries to investigate the effect of radiation through the glasses. Table 10 shows the transmissivity coefficients (Tr) for each glass boundary. Solar radiation decomposed of three spectrum bands which are ultraviolet (UV), visible light and infrared (IR).

Table 10. Transmissivity coefficients of glass boundaries for baseline and modified scenarios.

Scenario	Boundary	Transmissivity UV	Transmissivity visible light	Transmissivity IR
Baseline*	Windshield Front side windows	10 %	90%	83%
	Rear window Rear side windows	30%	90%	83%
Modified glass**	Windshield Front side windows	10%	75%	35%
	Rear window Rear side windows	10%	30%	10%

*: Based on the values of normal vehicle window characteristics.

**: Based on the possible solutions

Figure 35 below shows the implemented transmissivity coefficients in Star-CCM+ program.

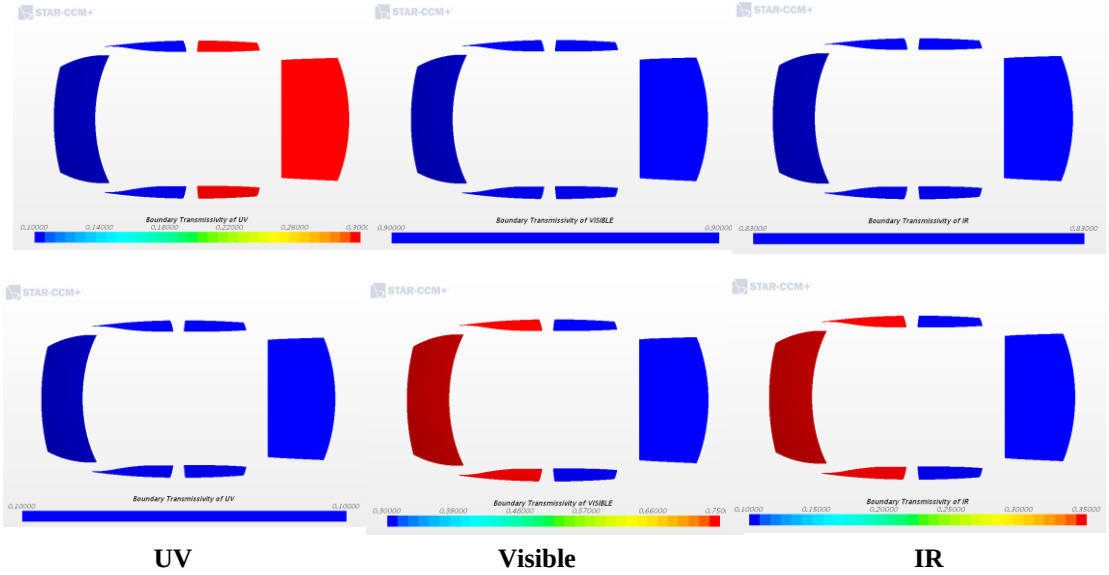

Figure 35. Boundary condition of transmissivity for windows for baseline (up) and tinted glass (down).

6.4.2 Heating Mode

In order to heat up the air inside the cabin, warm air is supplied to the cabin volume through windshield defroster, side vents, front and rear floor vents. Baseline and modified cases are defined to investigate the effect of double-pane glass on the cabin air condition. Table 11 shows the boundary conditions for cooling mode.

Table 11. Boundary conditions for cooling mode.

Boundary	Boundary type	Physics value	Temperature
Windshield defroster	Volume flow	33.8 l/s	33 C
Side vents	Volume flow	15.4 l/s	33 C
Front floor vent	Volume flow	31 l/s	33 C
Rear floor vent	Volume flow	20.5 l/s	33 C
Total	Volume flow	100 l/s	-

Additional boundary conditions are defined for the glass boundaries to investigate the effect of double glazing on the glasses as shown in figure 36.

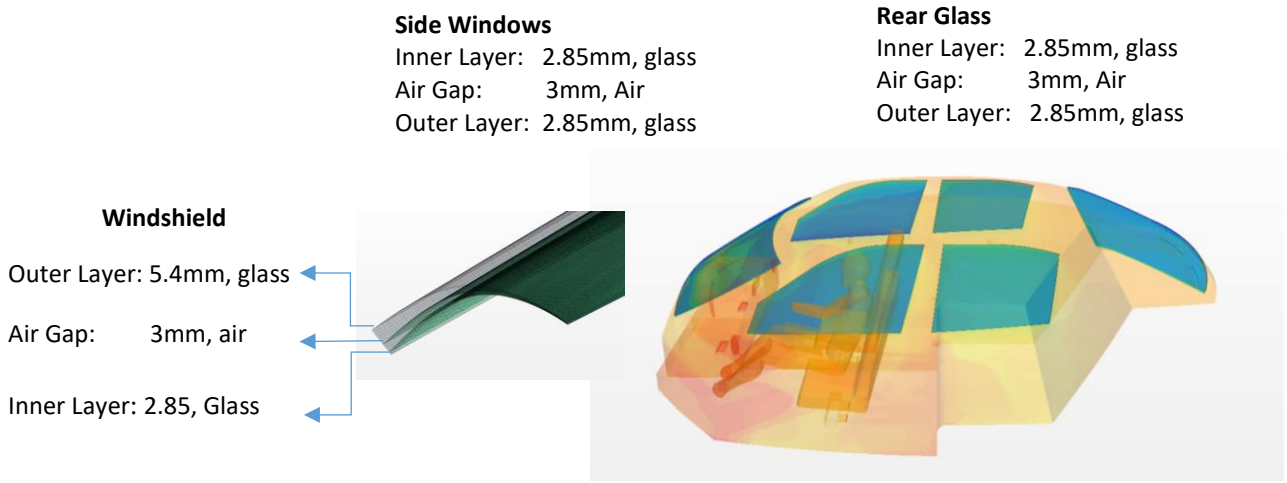

Figure 36. Boundary conditions of double-pane glass.

7 RESULTS OF CABIN 3D SIMULATION

This chapter presents the results of 3D simulation in Star-CCM+ program based on the model and boundary conditions defined in chapter 6 of this thesis. The results are categorized in two sections of cooling and heating modes.

7.1 Cooling mode

In this mode of air conditioning, the ambient temperature is +30℃ and cabin boundaries are exposed to solar radiation as described in section 6.1 above. Presented results in cooling mode are heat flux over the windows and temperature distribution in cabin air volume.

7.1.1 Heat Flux Over the Windows

Figures 37 and 38 below show the heat flux to the cabin volume over the windows for the baseline and tinted scenarios. In tinted glass the heat flux significantly drops due to prevention of solar irradiation.

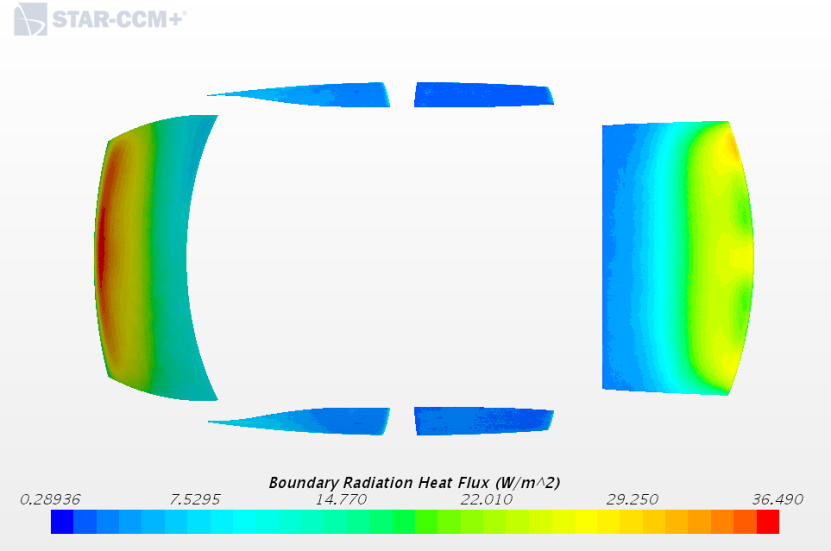

Figure 37. Boundary radiation heat flux for baseline scenario.

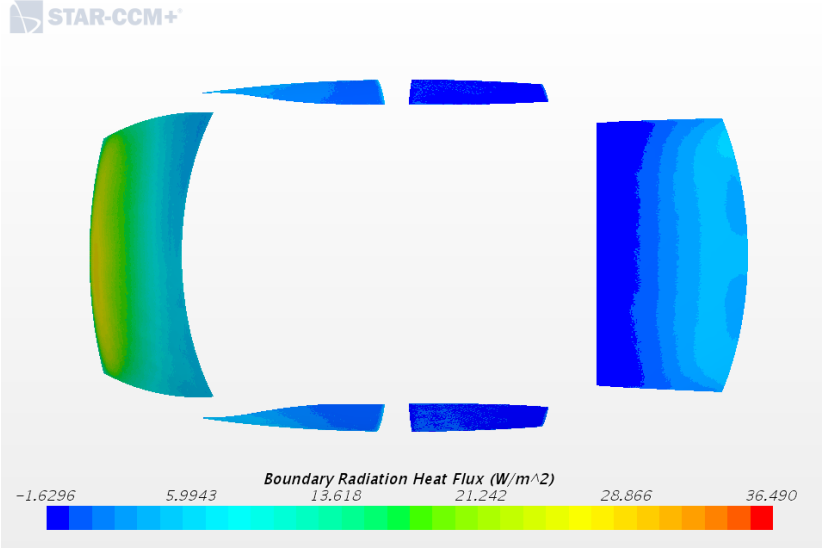

Figure 38. Boundary radiation heat flux for tinted glass scenario.

7.1.2 Temperature Distribution in Cabin Air Volume

The secondary objective for the tinting solution is to provide more uniform temperature distribution inside the cabin air volume. Figures 39 and 40 show the measuring points and temperature distribution inside the cabin air volume. For the tinted solution, the temperature at the front passenger breath points is less than the baseline case. In addition, it should be considered that in the tinted case, the temperature at the inlets is 3℃ less than the baseline.

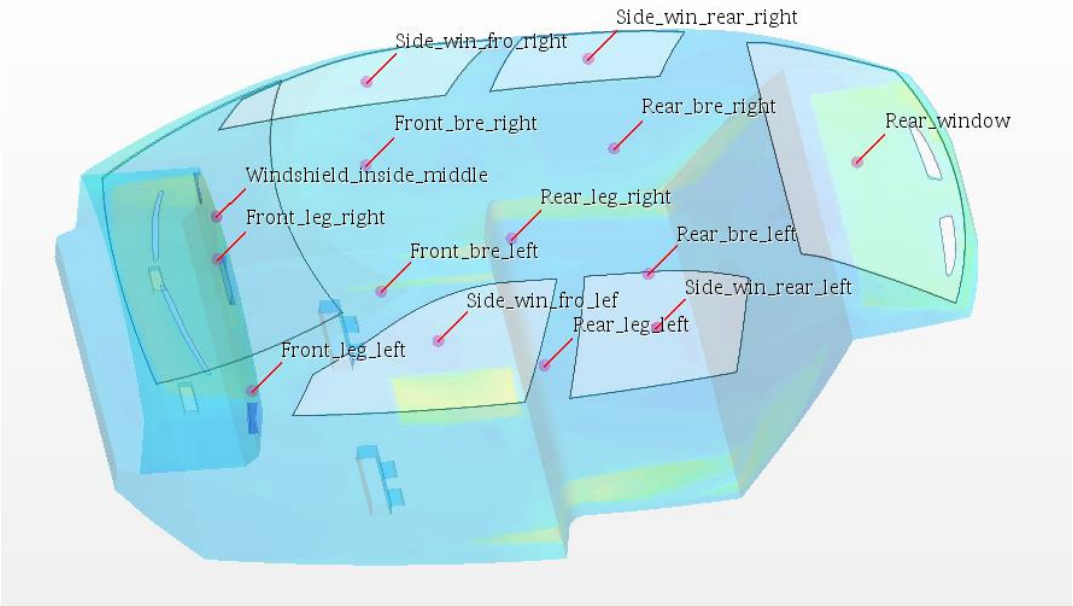

Figure 39. Measurement points for temperature distribution inside cabin air volume.

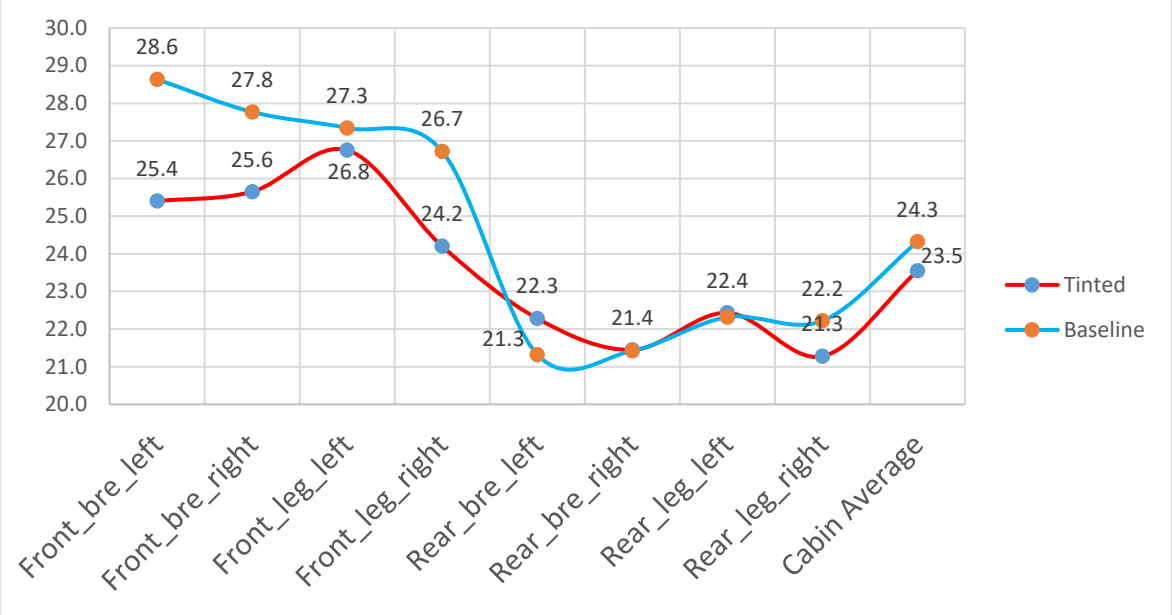

Figure 40. Temperature distribution of cabin air volume for cooling mode.

7.2 Heating Mode

In this mode of air conditioning, the ambient temperature is -10℃ and solar radiation is ignored to prepare the coldest possible case. Presented results in heating mode are heat rate over the windows and temperature distribution in cabin air volume.

7.2.1 Heat Transfer Through Windows

The primary objective of utilizing double-pane glass in this study is to decrease convective heat transfer through the windows. Figure 41 demonstrates the heat transfer rate at outer surface of double-pane glass in heating mode.

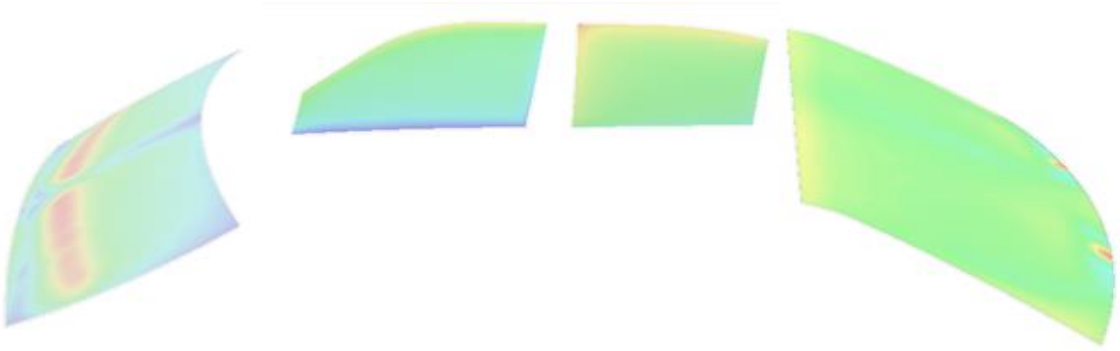

Figure 41. Heat transfer rate at inner layers in heating mode.

Table 12 below shows the average surface temperature of each boundary in heating mode.

Table 12. Average surface temperature of window layers.

Temperature	Windshield	Front side windows	Rear side windows	Rear windshield
Inner layer	+8.9 ℃	+1.6 ℃	+3.2 ℃	+2.9 ℃
Air gap	+0.1 ℃	-2.7 ℃	-1.6 ℃	-2.7 ℃
Outer layer	-8.6 ℃	-8.9 ℃	-8.8 ℃	-8.9 ℃

7.2.2 Temperature Distribution in Cabin Air Volume

The same as the cooling mode, the secondary objective in heating mode is to obtain more uniform temperature inside the cabin while decreasing the total energy demand. Figure 42 below depicts the temperature distribution inside the cabin for selected points.

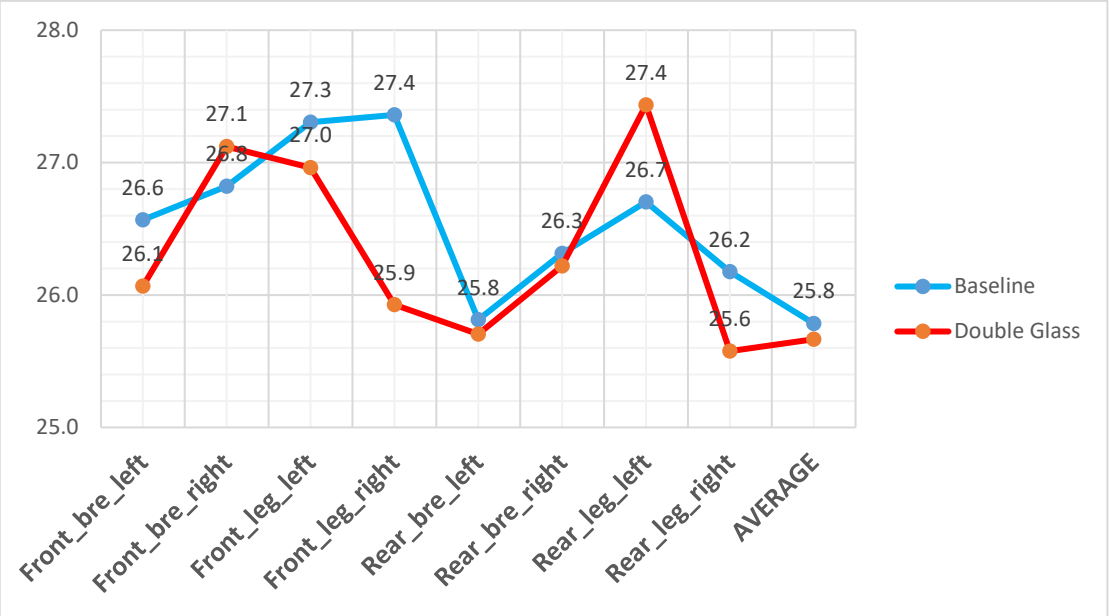

Figure 42. Temperature distribution inside the cabin air volume for heating mode.

7.2.3 Energy Saving

The primary objective of this study is to maintain the comfortable air condition in the cabin while saving energy. The energy saved in each mode is calculated based on difference in energy supplied to the cabin in baseline and modified scenarios.

Table 13. Total energy rate saving in cooling and heating modes.

HVAC mode	Energy saving
Cooling	230 W
Heating	180 W

8 CONCLUSION

This chapter compares the baseline scenario and proposed solutions for both cooling and heating modes. As described in chapter 7, double glazing and glass tinting will help to decrease the energy consumption for both heating and cooling. Additionally, relevant criteria in each case is added to comparison matrix.

8.1 Double-pane Glass

Table 14 shows the assessment of double-pane glass in terms energy saving, availability of technology, noise reduction, safety, weight and battery range.

Table 14. Assessment of double-pane glass.

Criteria	**Double-pane glass**		
	Advantage	Disadvantage	Details
Energy saving	✔		Saves 180 W power by decreasing heat transfer rate through glasses
Availability of technology	✔		Utilized by other companies
Environmental noise reduction	✔		
Safety	✔		
Weight		✔	~15 Kg weight increase (excluding front windshield)
Battery Range	✔	✔	Saves thermal energy also increases total weight

8.2 Tinted Glass

For the side and rear windows, the effect of tinted-glass glass is investigated. Relevant criteria are energy saving, passengers' overall comfort, material recovery and battery range.

Table 15. Assessment of tinted glass.

Criteria	**Tinted glass**		
	Advantage	Disadvantage	Details
Energy saving	✔		Saves 230 W power by decreasing transparency of glasses
Passengers comfort	✔		Reduces unwanted solar radiation
Material recovery		✔	Mixes plastic and glass layer
Battery Range	✔		Reduces required cooling power

8.2.1 Conventional Tinting

This section compares 4 tinting solutions which are available in the market. Dyed window tinted glass, metallized solar film, IR carbon and transparent film are four typical tinting options available in the market. The structure of tinting layer is defined in figure 43 below.

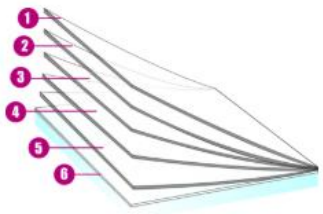

Figure 43. Construction of tinting layer. (Solarscreen.eu, 2018)

The layers of tinting film are:

1. Scratch resistant layer, increases durability and rigidity
2. Colored polyester
3. Adhesive
4. Colored polyester
5. Pressure-sensitive adhesive, forms a glass bond in 15 days
6. Protection layer, disposed after installation

Table 16 below illustrates the characteristics of different tinting solutions.

Table 16. Properties of conventional tinting solutions*. (Solarscreen.eu, 2018)

Conventional tinting solutions	**Dyed window tint film**	**Metallized**	**IR Carbon**	**Transparent**
Ultraviolet transmission	1 %	1 %	1 %	<1 %
Visible light transmission	6-70 %	3-70 %	3-50 %	86 %
Reflection of external visible light	5-7 %	6-11 %	7-8 %	6 %
Total solar energy rejected	22-40 %	32-69 %	35-65 %	31 %
PET / PVC composition	PET	PET	PET	PET
Thickness	25-60 μ	55-65 μ	40-50 μ	60-180 μ
Color	BLACK	BLACK - SILVER	BLACK	HIGHLY NEUTRAL
Fire-resistance rating	-	M1	-	-

*Data calculated based on film applied to clear glass 3 mm thick (on double glazing 4-16-4)

The major difference of the presented solutions are the materials used as radiation barriers. Table 17 below compares the proposed solutions.

Table 17. Summary of conventional tinting solutions. (Solarscreen.eu, 2018)

Conventional tinting solutions	
Dyed window tint film	• The most economical type of window-tinting film • Solar heat is absorbed by the dye in the film • Primarily for appearance. • The dye does tend to fade with time. • The heat-reduction is not particularly high.
Metallised	• Small metallic particles reflect heat • Metallic content strengthens the window against shattering. • Shiny appearance from the outside. • It is more resistant to scratches than dyed film. • Metallic content interferes with cell phone GPS and radio reception.
IR Carbon	• Proper for cell phones and radio transmission (doesn't have any metal in it) • The carbon content inside the film blocks approximately 40% of the IR light.
Transparent (Ceramic)	• The highest quality and the most expensive window tint film • Prevents infra-red light (up to 50 %) • Maximum visibility both by day and night. • Resistant to glare and fading, and highly shatter-proof. • Most effective in blocking of ultraviolet light (up to 99%)

8.2.2 Interactive Glass

Smart multifunctional glass is new solution for both building and vehicle glass. This technology adds interconnectivity with a smart electronics system for application in vehicle. The basis lies in electrochromic (dynamic sunscreen) glass basically introduced for passengers' comfort and energy saving. (RISE Research Institutes of Sweden, 2018)

Figure 44. Interactive glass concept design. (RISE Research Institutes of Sweden, 2018)

8.2.3 Smart Tinting

Electronically dimmable windows are applicable for improving visual and thermal comfort inside the vehicle. Boeing has introduced automatic window dimming for its 787 Dreamliner. Controllable shading solution from clear to dark increases the comfort of passengers while blocking UV and rejecting heat. The current drawback of this technology is getting dark when electricity supply is disconnected. (Vision-systems.fr, 2018)

Figure 45. Electronically dimmable windows in airplane. (Vision-systems.fr, 2018)

9 SUMMARY

Thermal management system of an electric vehicle is simulated in 1D using GT-Suite program to identify the heat loss in each subsystem. Powertrain, traction batteries and passenger compartment are three main subsystems where heating and cooling in three use cases of 40, 80 and 120 kph are investigated.

Based on the results of the 1D analysis, glass boundaries of cabin have the highest heat loss and incorporate high potential for energy saving. Thereafter, two insulation solution for cooling and heating modes are proposed and investigated in 3D simulation using Star-CCM+ program. As the final step insulation solutions are compared regarding energy saving, weight and passenger comfort.

Both proposed solutions for vehicle glazing show good result in terms of energy saving. However, appropriate solution should embrace proper insulation for cooling along with heating mode. In the other hand use of air barrier as insulator for glass is a low price and effective way which can be used in future designs of vehicle. This concept is also compatible with interactive and smart tinting glass solutions for autonomous driving vehicles.

10 FUTURE WORKS

The author recommends the following tasks to be done in future works to develop this study.

10.1 Under-hood model Propulsion loop

The quasi 3D model of under-hood components developed during this project in Cool 3D environment. However, due to limitation in time and scope of the project, further works are halted. In other to integrate the whole system of EV it would be beneficial to add under-hood system to the other sub-systems of thermal management.

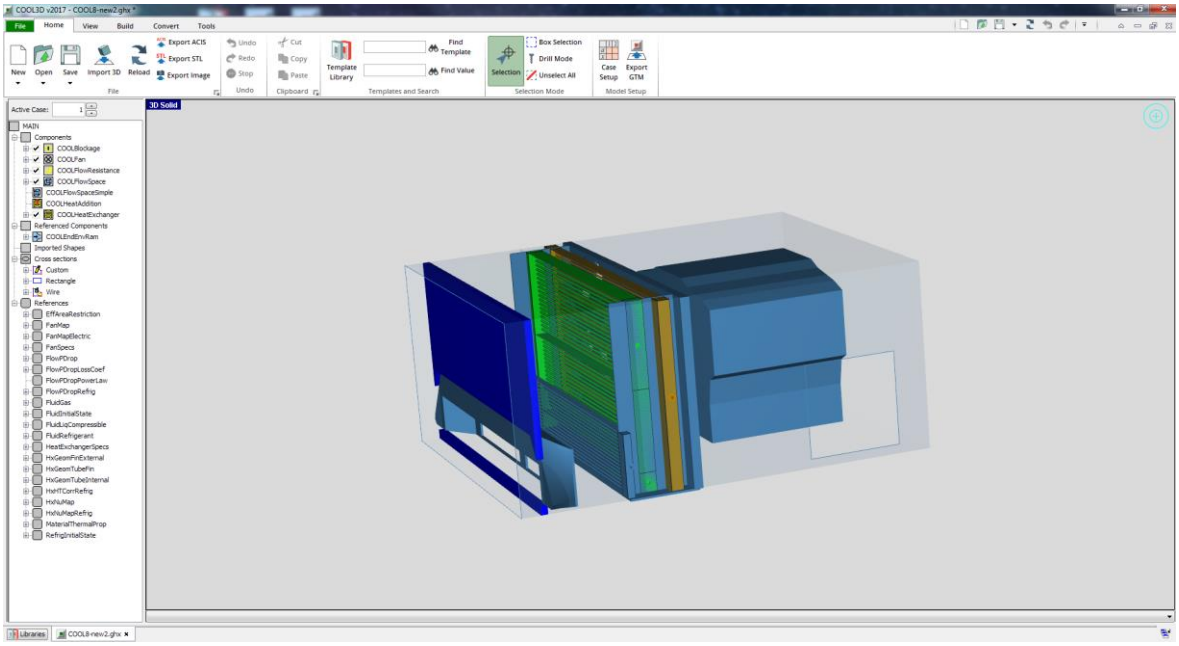

Figure 46. Quasi 3D model of underhood in Cool 3D.

10.2 Transient mode

The scope of this thesis project was to study the behavior of thermal system for all components and in steady state. However, it is beneficial to study the thermal system in transient state, where drive cycles and transient functionality of components is investigated.

10.3 Experimental confirmation

The result of 3D simulation should be compared with testing real components in wind tunnel. Therefore, temperature distribution in cabin and thermal performance of double-pane glass for vehicle should be investigated.

REFERENCES

Becker, T. and Sidhu, I. (2009). Center for Entrepreneurship & Technology (CET) Technical Brief. [Online] cet.berkeley.edu. Available at: http://globaltrends.thedialogue.org/wp-content/uploads/2014/12/Electric-Vehicles-in-the-United-States-A-New-Model-with-Forecasts-to-2030.pdf [Accessed 1 Apr. 2018].

Continental-automotive.com. (2018). Continental Automotive. [online] Available at: https://www.continental-automotive.com/en-gl/Passenger-Cars/Powertrain/Diesel-Technology/Thermal-Management/Electrical-Water-Pump [Accessed 26 Aug. 2018].

Chevrolet.com. (2018). 2019 Bolt EV Electric Car: An Affordable All-Electric Car. [online] Available at: https://www.chevrolet.com/electric/bolt-ev-electric-car [Accessed 10 Sep. 2018].

EEA. (2017). Final Energy Consumption by Mode of Transport. [Online] Available at: https://www.eea.europa.eu/data-and-maps/indicators/transport-final-energy-consumption-by-mode/assessment-8 [Accessed 28 Mar. 2018].

Ekh, Magnus and S. Toll. (2016). Mechanics of Solids & Mechanics of Fluids. introduction to continuum mechanics. [online] Available at http://www.tfd.chalmers.se/~lada/MoF/postscript/SF-I.pdf

Gamma Technologies. (2016). GT-ISE Tutorials v.7.0. Gamma Technologies Inc, 2016, 51 pp;

Lidar, J. (2018). Thermal Analysis of Engine Bay in Star-CCM+. Method Development and Correlation with Experimental Data.. [online] Chalmers studentarbeten. Available at: http://studentarbeten.chalmers.se/publication/254928-thermal-analysis-of-engine-bay-in-star-ccm-method-development-and-correlation-with-experimental-data [Accessed 10 Dec. 2018].

Nielsen, F. 2016. *Automotive Climate Systems - Investigation of Current Energy Use and Future Energy Saving Measures*. Thesis for the degree of Doctor of Philosophy. Chalmers

University of Technology, Department of Civil and Environmental Engineering. Gothenburg, Sweden.

Nissan Motor Co. (2018). e-Powertrain. [online] Nissan Technological Development Activities. Available at: https://www.nissan-global.com/en/technology/overview/e_powertrain.html [Accessed 22 Aug. 2018].

Jarrett, A. and Kim, I. (2011). Design optimization of electric vehicle battery cooling plates for thermal performance. Journal of Power Sources, 196(23), pp.10359-10368.

Porsche engineering magazine. (2011). Thermal management in vehicles with electric drive system. [online] Available at: https://www.porscheengineering.com/filestore/download/peg/en/pemagazin-01-2011-artikel-waermemanagementvonfahrzeugenmitelektrischemantrieb/default/78115e66-c26a-11e4-a19d-001a64c55f5c/Thermal-Management-in-Vehicles-with-Electric-Drive-System-Porsche-Engineering-Magazine-01-2011.pdf [Accessed 8 Feb. 2018].

Putra, N. 2017. Electric motor thermal management system using L-shaped flat heat pipes. Applied Thermal Engineering, 126, pp. 1156-1163.

Rauh, N., Franke, T. and Krems, J. (2014). Understanding the Impact of Electric Vehicle Driving Experience on Range Anxiety. Human Factors: The Journal of the Human Factors and Ergonomics Society, 57(1), pp.177-187.

RISE Research Institutes of Sweden. (2018). Multifunctional glass with integrated control system | RISE Research Institutes of Sweden. [online] Available at: https://www.ri.se/en/what-we-do/projects/multifunctional-glass-integrated-control-system [Accessed 10 Aug. 2018].

Sato, N. (2001). Thermal behavior analysis of lithium-ion batteries for electric and hybrid vehicles. Journal of Power Sources, 99(1-2), pp.70-77.

Siegel, R., Howell, J. and Mengüç, M. (2011). Thermal radiation heat transfer. 5th ed.

Smith, J., Hinterberger, M., Hable, P. and Koehler, J. (2014). Simulative method for determining the optimal operating conditions for a cooling plate for lithium-ion battery cell modules. Journal of Power Sources, 267, pp.784-792.

Solarscreen.eu. (2018). FILMS - Automotive. [online] Available at: https://www.solarscreen.eu/films/en/9/automotive [Accessed 21 Sep. 2018].

Stutenberg, K. (2014). Advanced Technology Vehicle Lab Benchmarking – Level 1. [Online] U.S. Department of Energy. Available at: https://www.energy.gov/sites/prod/files/2014/07/f17/vss030_stutenberg_2014_o.pdf [Accessed 7 Mar. 2018].

Valeo. (2018). Air-conditioning loop: Valeo, spare parts conception for thermal system efficiency. [online] Available at: http://www.valeo.de/en/our-activities/thermal-systems/technologies/air-conditioning-loop-373.html [Accessed 20 Sep. 2018].

Valeo. (2018). Cabin filters: Valeo, spare parts conception for thermal system efficiency. [online] Available at: http://www.valeo.de/en/our-activities/thermal-systems/technologies/cabin-filters-374.html [Accessed 20 Sep. 2018].

Vepsäläinen, A., Pitkänen, J. and Hyppänen, T. (2012). FUNDAMENTALS OF HEAT TRANSFER. Lappeenranta: Lappeenranta University of Technology.

Versteeg, H. and Malalasekera, W. (2007). An introduction to computational fluid dynamics. 2nd ed. Harlow, England: Pearson Education Ltd., pp.472-494.

Vision-systems.fr. (2018). Vision Systems | Architect of innovations. [online] Available at: http://www.vision-systems.fr/ [Accessed 10 Aug. 2018].